A Rho family GTPase controls actin dynamics and tip growth via two counteracting downstream pathways in pollen tubes

Ying Gu,[1,2] Ying Fu,[1,2] Peter Dowd,[3] Shundai Li,[1,2] Vanessa Vernoud,[1,2] Simon Gilroy,[4] and Zhenbiao Yang[1,2]

[1]Center for Plant Cell Biology, Institute for Integrative Genome Biology, and [2]Department of Botany and Plant Sciences, University of California, Riverside, Riverside, CA 92521
[3]Department of Biochemistry and Molecular Biology and [4]Department of Biology, Pennsylvania State University, State College, PA 16802

Tip growth in neuronal cells, plant cells, and fungal hyphae is known to require tip-localized Rho GTPase, calcium, and filamentous actin (F-actin), but how they interact with each other is unclear. The pollen tube is an exciting model to study spatiotemporal regulation of tip growth and F-actin dynamics. An *Arabidopsis thaliana* Rho family GTPase, ROP1, controls pollen tube growth by regulating apical F-actin dynamics. This paper shows that ROP1 activates two counteracting pathways involving the direct targets of tip-localized ROP1: RIC3 and RIC4. RIC4 promotes F-actin assembly, whereas RIC3 activates Ca^{2+} signaling that leads to F-actin disassembly. Overproduction or depletion of either RIC4 or RIC3 causes tip growth defects that are rescued by overproduction or depletion of RIC3 or RIC4, respectively. Thus, ROP1 controls actin dynamics and tip growth through a check and balance between the two pathways. The dual and antagonistic roles of this GTPase may provide a unifying mechanism by which Rho modulates various processes dependent on actin dynamics in eukaryotic cells.

Introduction

Tip growth is fundamentally important for the development and morphogenesis of all eukaryotic organisms. This extremely polarized growth is dependent on targeted exocytosis in the apical region of the cell, allowing the generation of tubular structures such as neuronal axons in animals, hyphae in fungi and pollen tubes, and root hairs in higher plants. Several common features exist in tip growth among these different systems: (a) growth occurs rapidly over a long distance; (b) the cell apex is capable of sensing directional cues to redirect growth; and (c) the dynamics of F-actin and Ca^{2+} are required. Single-celled yeast, a model system for the study of polarized growth, shares some but not all of these features; but it is not clear whether or not the yeast paradigm for polarized growth is applicable to tip growth in higher multicellular organisms. Consequently, the mechanism for tip growth in higher eukaryotes is not well understood.

The pollen tube of higher plants is a fascinating model system for the study of tip growth and thus has attracted broad interest and intense scrutiny for many years (Franklin-Tong, 1999; Zheng and Yang, 2000; Hepler et al., 2001; Johnson and Preuss, 2002; Lord and Russell, 2002). During pollination, pollen grains are deposited on the surface of the stigma (pollen-receiving part of the female pistil in flowers) and communicate with the stigma to select a site for germination. Once germinated, pollen generates a tube that travels along a tortuous path to the ovule where sperm are delivered to the egg cell. This guided tip growth is analogous to neuronal axon targeting (Palanivelu and Preuss, 2000; Lord, 2003; Yang, 2003). Pollen tube growth and axon development and guidance apparently share remarkable similarities in the underlying molecular and cellular mechanisms. For example, Rho family GTPases, Ca^{2+} fluctuations, and actin dynamics all play important roles in these processes (Hepler et al., 2001; Fu et al.; 2001; Vidali et al., 2001; McKenna et al., 2004). However, the mechanistic linkage among these events is unknown in these systems.

ROP1, belonging to the Rho family of small GTPases including Rho, Cdc42, and Rac, is a central regulator of tip growth in pollen tubes (Lin and Yang, 1997; Kost et al., 1999; Li et al., 1999). Tip-localized ROPs are essential for tube elongation and the control of growth polarity. Pollen tube growth is blocked by depletion or inhibition of *ROP1*, whereas expression of constitutively active mutants of *ROP1* induces growth depolarization (i.e., bulbous tubes or tip swelling; Lin and Yang, 1997; Kost et al., 1999; Li et al., 1999). ROP1 regulates the dynamics of

Correspondence to Z. Yang: zhenbiao.yang@ucr.edu

Abbreviations used in this paper: CRIB, Cdc42/Rac interactive binding; FRET, fluorescence resonance energy transfer; LatB, latrunculin B; LOF, loss-of-function; OX, overexpression; PM, plasma membrane; WT, wild-type.

The online version of this article includes supplemental material.

Supplemental material can be found at:
http://doi.org/10.1083/jcb.200409140

The Journal of Cell Biology, Vol. 169, No. 1, April 11, 2005 127–138
http://www.jcb.org/cgi/doi/10.1083/jcb.200409140

F-actin in the tip and possibly Ca^{2+} signaling as well (Li et al., 1999; Fu et al., 2001). ROP1 inactivation eliminates a tip-focused Ca^{2+} gradient essential for pollen tube growth and alters pollen tube growth responses to extracellular Ca^{2+} (Pierson et al., 1994; Malho and Trewavas, 1996; Li et al., 1999). ROP1 inactivation also depletes apical F-actin, whereas *ROP1* overexpression (OX) induces both the stabilization of this F-actin and the depolarization of growth. The *ROP1* OX–induced growth depolarization is suppressed by latrunculin B (LatB), an actin-depolymerizing drug, indicating that ROP-dependent actin dynamics are critical for tip growth (Fu et al., 2001).

Actin dynamics play a fundamental role in many processes in all eukaryotic organisms; e.g., neuron development, growth, and guidance; cell polarity, growth, and movement; and gene expression (Dickson, 2001; Luo, 2002; Miralles et al., 2003; Pollard and Borisy, 2003). For example, the axonal growth cone motility that involves constant extrusion and retraction of filopodia and lamellipodia is controlled by the dynamics of cortical fine F-actin (Dickson, 2001). In most cases, actin dynamics involve Rho family GTPase-mediated actin assembly and its disassembly promoted by ADF, gesolin, and/or profilin (Etienne-Manneville and Hall, 2002; Pollard and Borisy, 2003).

In this paper, we demonstrate that ROP1 GTPase controls actin dynamics in pollen tip growth via two coordinately counteracting pathways controlled by the ROP1 targets RIC3 and RIC4. The RIC4 pathway promotes the assembly of the apical F-actin, whereas the RIC3 pathway promotes disassembly of this actin via a Ca^{2+}-dependent process. Furthermore, these pathways regulate each other to control actin dynamics and tip growth. To our knowledge, this is the first demonstration of a Rho GTPase signaling network with two antagonistic pathways acting coordinately to control actin dynamics and tip growth, providing important new insights into the mechanism underlying these fundamental processes in higher eukaryotic organisms.

Results

RIC3 and RIC4 are two distinct ROP1 target proteins

To understand how ROP1 regulates pollen tube growth, we investigated a class of putative ROP1 effector proteins from *Arabidopsis thaliana*, termed RICs (ROP-interactive CRIB-containing proteins; Wu et al., 2001). RICs are novel proteins that share a Cdc42/Rac interactive binding (CRIB) motif, which is present in many Cdc42/Rac effectors and responsible for their specific interaction with activated Cdc42/Rac (Burbelo et al., 1995; Aspenstrom, 1999). Among nine *RICs* expressed in *A. thaliana* pollen, only *RIC3* or *RIC4* OX induced depolarized growth in tobacco pollen tubes as did *ROP1* OX, suggesting that these two RICs, but not other RICs, may be ROP1 targets to control polarized tip growth in pollen tubes (Wu et al., 2001).

If RIC3 and RIC4 are ROP1 targets, they are expected to bind active ROP1 and to display ROP1 activation-dependent localization and function. In vivo ROP1 interaction with RIC3 or RIC4 was tested using fluorescence resonance energy transfer (FRET) analysis of tobacco pollen tubes coexpressing *CFP-ROP1* and *YFP-RIC3* or *YFP-RIC4* fusion genes. As shown in Fig. 1 A, YFP-RIC4 or -RIC3 signals were detected when tubes were excited with a laser that excites CFP but not YFP, indicating FRET was occurring. The same settings did not detect any YFP signals in tubes expressing CFP-ROP1/YFP, CFP/YFP-RIC4, or CFP/YFP-RIC3 (unpublished data). FRET between CFP-ROP1 and YFP-RIC3 or -RIC4 was further con-

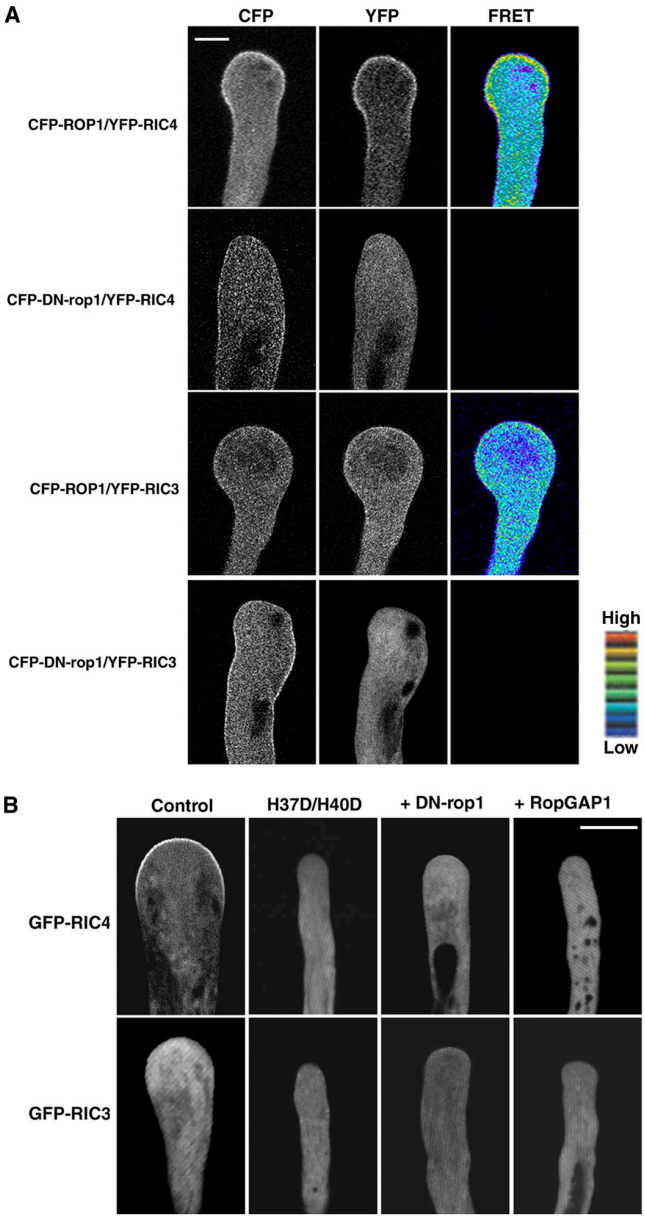

Figure 1. **RIC3 and RIC4 are direct targets of ROP1 GTPase.** (A) FRET analysis of in vivo ROP1 interaction with RIC3/RIC4. Tobacco pollen tubes coexpressing CFP-ROP1 or -DN-rop1 and YFP-RIC3 or -RIC4 were analyzed as described in the text. A pseudo-color scale with the intensity of FRET signals is displayed in the right panel (red, highest signal). All images were mid-plane sections. Bar, 10 μm. (B) Tip localization of RIC3/RIC4 requires their interaction with active ROP1. Control shows typical GFP-RIC4 or -RIC3 localization and tip morphology in tobacco pollen tubes transiently expressing *LAT52:GFP-RIC4* or *-RIC3*, respectively. H37D/H40D shows tobacco tubes transiently expressing GFP-tagged RIC3 or RIC4 mutant (mutations in the two conserved histidine residues in the CRIB motif). DN-rop1 or RopGAP1 shows tubes coexpressing GFP-RIC3 or -RIC4 with DN-rop1 or RopGAP1, respectively. All images were mid-plane confocal optimal sections. Bar, 15 μm.

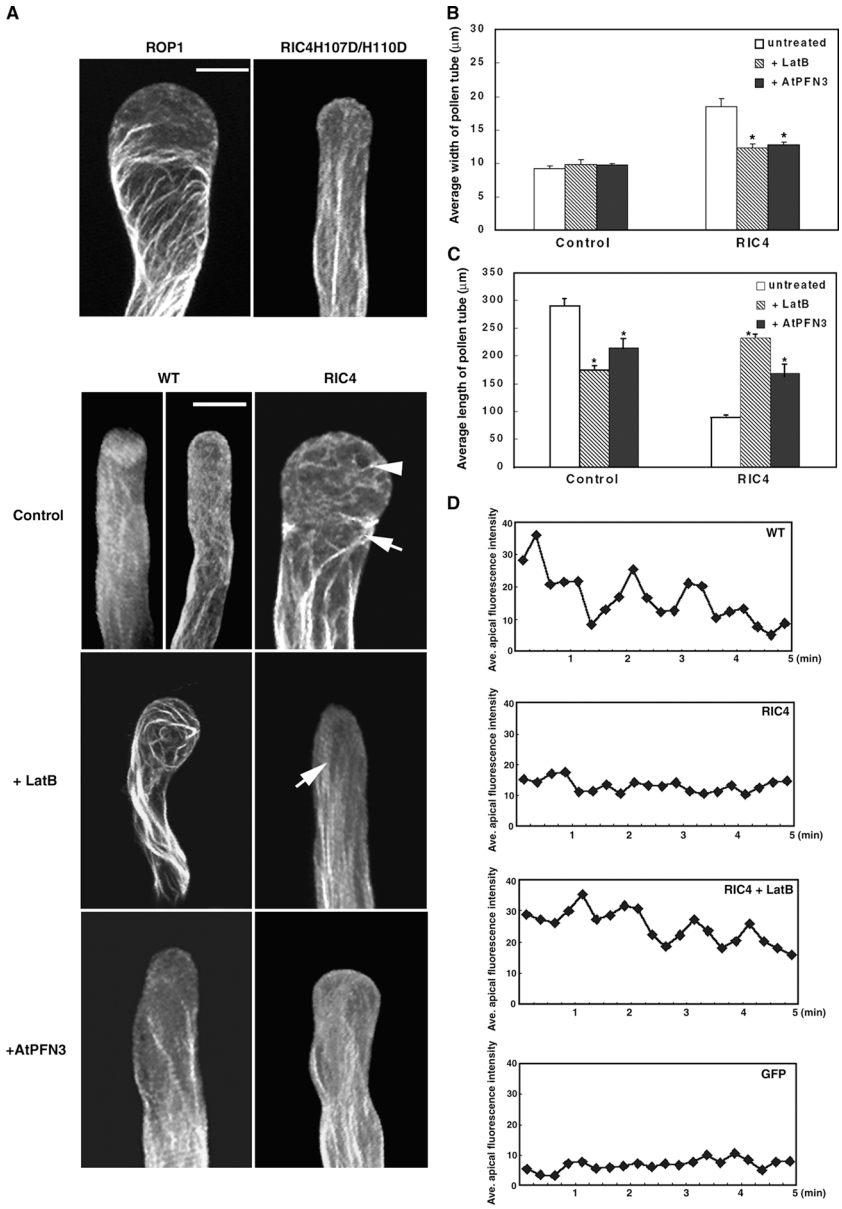

Figure 2. **RIC4 promotes the assembly of dynamic tip F-actin.** (A) *RIC4* OX induced a stable F-actin network at the tip that was reversed by LatB or profilin. *LAT52:GFP-mTalin* was transiently expressed alone or coexpressed with *LAT52:RIC4*, *LAT52:ROP1*, or *LAT52:RIC4H107DH110D* in tobacco pollen tubes gown in the presence of 10 μM Ca^{2+}. 5 h after bombardment, tubes were treated with 5 nM LatB for ~1 h. For profilin experiments, *LAT52:AtPFN3* was cooverexpressed with *LAT52:GFP-mTalin* and *LAT52:RIC4* in untreated tubes. GFP-mTalin was analyzed by confocal microscopy as described previously (Fu et al., 2001). All images shown are projections of 1-μm sections. Arrowhead points at the stable actin network at the tip. Arrow indicates the end of the actin cables. Bar, 10 μm. A video (Video 1) showing the stable actin network is presented in the online supplemental material. (B and C) LatB or AtPFN3 suppressed *RIC4* OX–induced depolarization of tobacco pollen tubes. All experiments were performed as described in A, and the maximum tip width and the length of pollen tubes were measured 1 h after LatB treatment or 6 h after bombardment. Data were collected from three individual experiments (~50 tubes per experiment). Asterisk indicates a significant difference from WT at the same data point ($P < 0.05$; *t* test). (D) *RIC4* OX–induced disruption of apical actin oscillation is suppressed LatB. Control (WT) and treatment experiments were performed as described in A. A time series (15-s intervals) of mid-plane confocal sections of tubes expressing GFP-mTalin was taken, and the average GFP intensity in a region of the apical dome (~5 μm from the extreme apex) was determined as described previously (Fu et al., 2001). Normalized average GFP intensity was used to represent relative amounts of F-actin at the tip. Y axis values are arbitrary units of the normalized GFP intensity; x axis indicates time (min) starting from the first collected image. Cytosolic GFP was used as a negative control showing no significant oscillation of fluorescence in the identical region of the tube measured for GFP-talin oscillation.

firmed by acceptor photobleaching experiments, in which an increase in CFP-ROP1 signal was detected when YFP-RIC fluorescence was bleached (unpublished data). No FRET signals were detected when CFP-ROP1 was replaced with CFP-DN-rop1, a dominant-negative T20N mutant of ROP1 (Li et al., 1999; Fig. 1 A). Furthermore, no FRET occurred when CFP-ROP1 and YFP-RIC3 or -RIC4 were coexpressed with RopGAP1 (ROP GTPase-activating protein 1; unpublished data), which deactivates ROP1 (Wu et al., 2000). Finally, no FRET signals were detected between ROP1 and another plasma membrane (PM)–targeted ROP, ROP10, showing that FRET does not occur between two noninteracting PM-localized proteins (unpublished data). These results indicate that RIC3 and RIC4 specifically interact with active ROP1 in vivo.

The CFP-ROP1/YFP-RIC4 FRET signals were preferentially distributed to the apical region of the PM (Fig. 1 B), similar to the GFP-RIC4 localization (Wu et al., 2001). CFP-ROP1/YFP-RIC3 FRET signals were slightly stronger in the apical region of the PM compared with the cytoplasm (Fig. 1 B), whereas GFP-RIC3 is preferentially localized to the apical region of the cytoplasm (Wu et al., 2001). This difference could be explained by rapid dissociation of activated RIC3 from the PM-localized GTP-bound ROP1. Nonetheless, these results suggest that the apical localization of RIC3 and RIC4 involves their interaction with activated ROP1.

We further examined if the apical RIC localization requires its interaction with ROP1. Mutations in two conserved histidine residues in the CRIB motif (H37D/H40D) in RIC1 abolished its interaction with ROP1 in vitro (Wu et al., 2001). As shown in Fig. 1 B, similar mutations eliminated the preferential localization of GFP-RIC3 to the cytoplasmic region behind the apical dome as well as the PM localization of GFP-RIC4. Furthermore, these mutations abolished the ability of RIC3 or RIC4 to induce tip swelling (Fig. 1 B). Overexpressing either *RopGAP1* or *DN-rop1* effectively caused GFP-RIC3 or GFP-RIC4 to uniformly localize to the cytosol like soluble GFP alone (Fig. 1 B). Furthermore, *RopGAP1*

suppressed GFP-RIC3– or GFP-RIC4–induced growth depolarization by reducing the enhanced width of *GFP-RIC3*–overexpressing tubes (from 14.7 to 9.2 μm; $n = 22$) and *GFP-RIC4*–overexpressing tubes (from 18.4 to 8.9 μm; $n = 27$). *DN-rop1* reduced the width of *GFP-RIC3*–overexpressing tubes from 14.7 to 12.3 μm ($n = 25$) and *GFP-RIC4*–overexpressing tubes from 18.4 to 13.8 μm ($n = 23$). All the differences were statistically significant ($P < 0.05$, Student's *t* test). Thus, ROP1 activation is required for RIC3 and RIC4 localization and function. Together, we conclude that RIC3 and RIC4 are both ROP1 targets in the control of pollen tube tip growth.

Because several other ROPs (ROP8–11) functionally distinct from ROP1 are also expressed in *A. thaliana* pollen, we tested whether RIC3 or RIC4 could act as targets of these ROPs (Fig. S1 and Table S1, available at http://www.jcb.org/cgi/content/full/jcb.200409140/DC1). Unlike ROP1, none of these ROPs altered GFP-RIC3 or -RIC4 localization when overexpressed, indicating that in cultured pollen tubes RIC3 and RIC4 are specific functional targets of ROP1 in the control of polarized tip growth but not of other pollen-expressed ROPs functionally distinct from ROP1.

RIC4 promotes the assembly of apical F-actin

Because tip-localized ROP1 regulates the dynamics of apical F-actin (Fu et al., 2001), we tested whether a RIC3 or RIC4 is involved in this aspect of ROP action. A GFP-tagged actin-binding domain of mouse talin (GFP-mTalin) decorated two distinct forms of F-actin in tobacco pollen tubes: axial cables that extend throughout the tube but end behind the tip of growing tubes and some form of dynamic tip F-actin (Fu et al., 2001). The GFP-mTalin–labeled apical structure seems to consist of short bundles at the extreme apex, apparently alternating with a collarlike structure a few micrometers back from the extreme apex (Fu et al., 2001; Fig. 2 A). The exact configuration of this tip actin structure remains to be determined because GFP-mTalin binding to F-actin might alter its configuration; so this form of F-actin is vaguely referred to as tip F-actin hereafter. Nonetheless, *RIC4* and *RIC3* OX induced distinct changes in apical GFP-mTalin labeling patterns in tobacco pollen tubes (Fig. 2 A vs. Fig. 4 A). *RIC4* OX converted the dynamic tip F-actin into a dense F-actin network, but did not change the axial actin cables (Fig. 2 A; 90% tubes, $n = 21$). Quantitative analysis shows that RIC4 OX resulted in a significantly greater amount of F-actin at the tip than control tubes (Fig. S2, available at http://www.jcb.org/cgi/content/full/jcb.300409140/DC1). The change in the tip F-actin was similar to that caused by *ROP1* OX, except that *RIC4* OX did not induce abnormal subapical actin hoops seen in *ROP1*-overexpressing tubes (Fu et al., 2001). Mutations in two conserved histidine residues in the CRIB motif (H107D/H110D) eliminate the ability of RIC4 to affect tip F-actin (Fig. 2 A), indicating that RIC4 interaction with active ROP1 is critical for its regulation of actin organization.

To test whether the *RIC4*-induced stable F-actin network was the effect or the cause of growth depolarization, *RIC4*-overexpressing tubes were treated with LatB, which partially suppresses the *ROP1* OX phenotype (Fu et al., 2001). LatB recovered normal apical F-actin and tip growth in the majority (85%, $n = 52$) of *RIC4*-overexpressing tubes (Fig. 2, A–C; and Fig. S2). Similarly, cooverexpression of AtPFN3, a G-actin sequestering protein expressed in pollen, suppressed both depolarized growth and the apical actin network induced by either *ROP1* (not depicted) or *RIC4* OX (Fig. 2, B and C). Compared with LatB, the recovery of tip growth by *AtPFN3* was only partial (80% tubes, $n = 50$), suggesting either that a factor that activates AtPFN3 is rate limiting or that another actin-depolymerizing factor coordinates with AtPFN3 in regulating actin dynamics.

Similar to *ROP1* OX (Fu et al., 2001), *RIC4* OX disrupted the oscillation of normal tip F-actin (Fu et al., 2001; Fig. 2 D). Furthermore, LatB recovered the oscillation of tip F-actin in *RIC4*-overexpressing tubes (Fig. 2 D; 92% tubes, $n = 51$). Together, our observations indicate that RIC4 promotes the assembly of tip F-actin in pollen tubes.

To further investigate the role of RIC4 in pollen tube growth, we isolated a loss-of-function (LOF) *ric4* mutant in *A. thaliana*, *ric4-1*, which contained a T-DNA insertion in the second intron and exhibited reduced *RIC4* mRNA level (Fig. 3

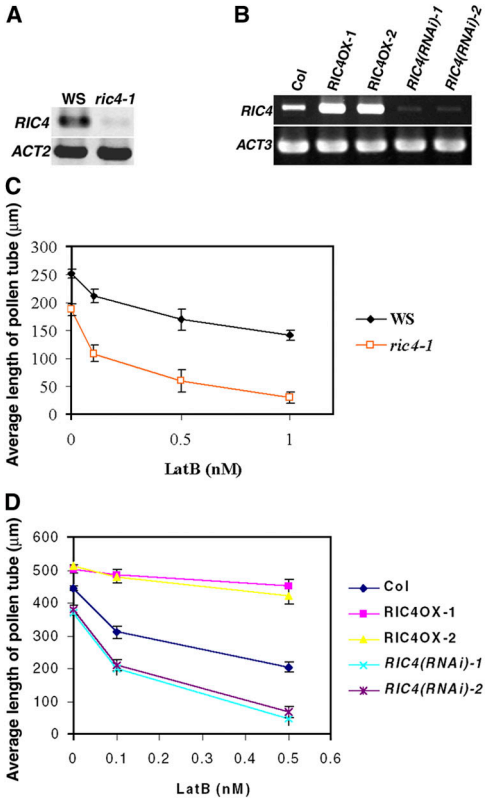

Figure 3. **The phenotypic characterization of *A. thaliana RIC4* mutant.** (A) RT-PCR analysis of *RIC4* mRNA expression in *ric4-1* in fluorescence tissues. WS, Wassilewskija WT. *ACTIN2* (*ACT2*) was used as a control for PCR amplification. (B) RT-PCR analysis of *RIC4* expression in *RIC4* OX and *RIC4(RNAi)*. Both OX and RNAi constructs were transformed into Columbia (Col) WT plants. RNA from mature pollen was used for RT-PCR analysis. *ACTIN3* (*ACT3*) was used as a control for PCR amplification. (C) The *ric4-1* pollen tubes are more sensitive to LatB inhibition of growth. (D) The effect of LatB on the growth of *RIC4* OX and *RIC4(RNAi)* pollen tubes. In both C and D, data were collected from three individual experiments (~100 tubes per experiment). The y axis represents average lengths of pollen tubes measured 9–12 h after germination, whereas the x axis represents the concentrations of LatB used. Error bars indicate standard errors.

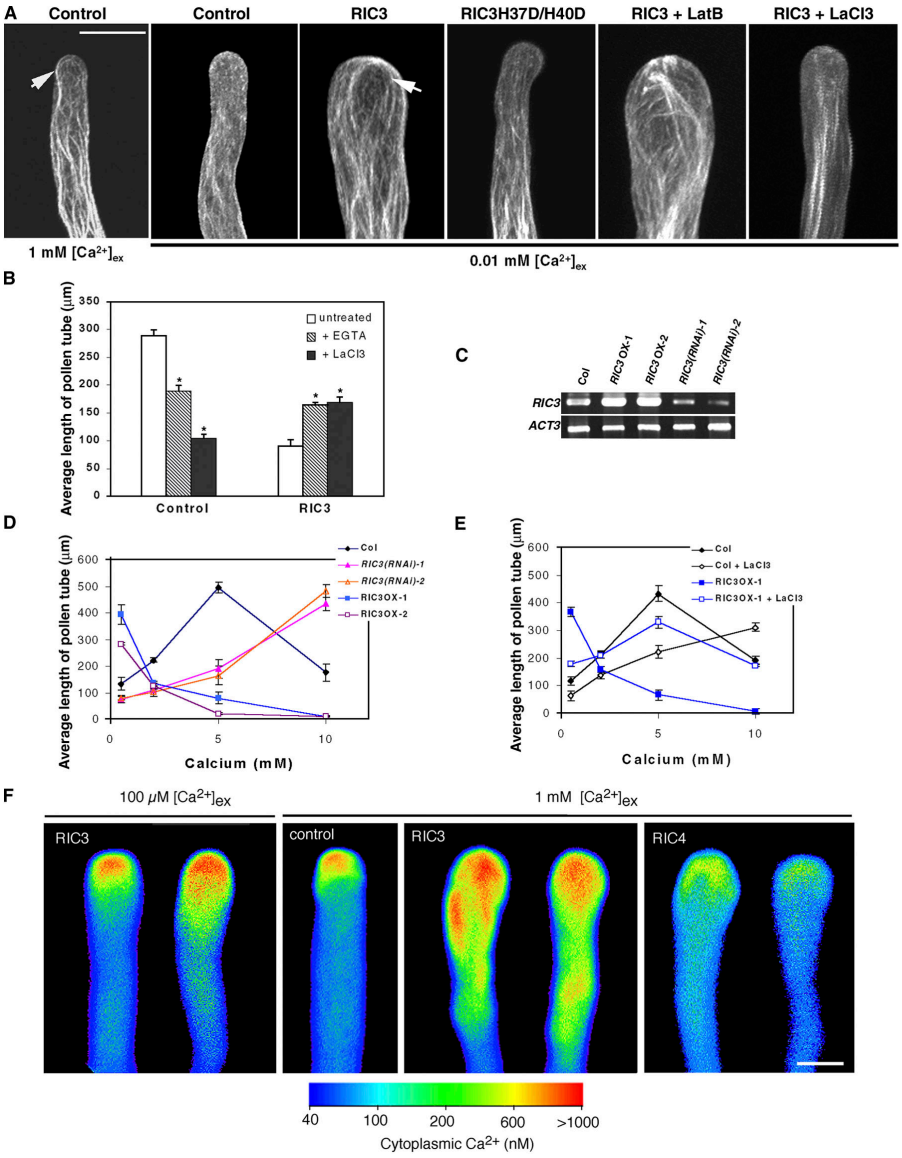

Figure 4. **RIC3 regulates Ca^{2+} signaling.** (A) *RIC3* OX–induced actin reorganization and depolarized growth were not suppressed by LatB. *LAT52:RIC3* was transiently coexpressed with *LAT52:GFP-mTalin* in tobacco pollen tubes grown in the presence of 10 μM Ca^{2+}. RIC3-overexpressing tubes were treated with 5 nM LatB (see Fig. 2 A) or with 100 μM $LaCl_3$ (see panel B). Control tubes (expressing *LAT52:GFP-mTalin* alone) were cultured in the presence of 10 μM or 1 mM Ca^{2+}. All images were projections of 1-μm confocal optical sections. Arrow, actin cables. Bar, 15 μm. A video (Video 2) showing actin cables protruding to the tip is presented in the online supplemental material. (B) Both EGTA and $LaCl_3$ suppressed *RIC3* OX–induced growth inhibition. EGTA and $LaCl_3$ were included in growth medium at a final concentration of 1 mM and 100 μM, respectively. Data were collected from three individual experiments (~50 tubes per experiment). Asterisk indicates a significant difference from WT at the same data point ($P < 0.01$; *t* test). (C) RT-PCR analysis of *LAT52:RIC3* OX and *LAT52:RIC3(RNAi)* lines. RNA from mature *A. thaliana* pollen was used for RT-PCR analysis. *ACTIN3* (*ACT3*) was used as a control for PCR amplification. Col, Columbia WT. (D) Increasing $[Ca^{2+}]_{ex}$ suppressed *RIC3(RNAi)*-induced inhibition of pollen tube growth, whereas decreasing $[Ca^{2+}]_{ex}$ rescued tube growth inhibited by *RIC3* OX. Pollen grains from WT plants (Col) and plants homozygous for *RIC3* OX and *RIC3(RNAi)* were germinated overnight on a medium containing 0.5, 2, 5, or 10 mM Ca^{2+}. Data were collected from three individual experiments (≥100 tubes per experiment). (E) $LaCl_3$ restored the *RIC3* OX–induced shift of the Ca^{2+} response curve. $LaCl_3$ was added into growth medium in a final concentration of 100 μM. Data were collected and analyzed as describe in D. (F) *RIC3* OX sustained normal tip growth and tip-focused Ca^{2+} gradient at suboptimal $[Ca^{2+}]_{ex}$ (100 μM) but led to delocalization and expansion of the tip gradient and swelling of the tube apex at 1 mM $[Ca^{2+}]_{ex}$. Pollen from *Petunia inflata* was cobombarded with *LAT52:RIC3/LAT52:GFP* or *LAT52:RIC4/LAT52:GFP* and then germinated at the indicated $[Ca^{2+}]_{ex}$. Tubes were then microinjected with the Ca^{2+} sensing dye Indo-1-dextran and Ca^{2+} was monitored by confocal ratio imaging. Ca^{2+} levels have been pseudo-color coded according to the inset scale. Bar, 15 μm.

A). The *ric4-1* tubes were significantly shorter and were more sensitive to growth inhibition caused by LatB (0.1–0.5 nM) than wild-type (WT) tubes (Fig. 3 C). Additional LOF *ric4* lines were generated using an RNAi construct under the control of the pollen-specific *LAT52* promoter (Eyal et al., 1995). *RIC4* mRNA levels were dramatically reduced in several independent *RIC4(RNAi)* lines (Fig. 3 B). Pollen tube growth in these lines was inhibited and was hypersensitive to LatB as seen in *ric4-1* (Fig. 3 D), indicating that the *ric4-1* phenotype was not due to an extragenic second site mutation. These results show that RIC4 is important for pollen tube elongation.

ROP1 inactivation causes depletion of tip F-actin in tobacco pollen tubes (Fu et al., 2001). Similarly, *ric4-1* tubes contained less tip F-actin than WT tubes (Fig. S3, available at http://www.jcb.org/cgi/content/full/jcb.200409140/DC1). However, WT *A. thaliana* pollen tubes did not contain as conspicuous F-actin at the tip as do tobacco pollen tubes. This finding could be explained by greater actin disassembly and/or less actin assembly in *A. thaliana* pollen tubes, which is consistent with their slower growth, as compared with tobacco pollen tubes. Indeed, *RIC4* OX increased tip F-actin accumulation (Fig. S3), promoted pollen tube growth, and reduced LatB sensitivity (Fig. 3 D). These data suggest that actin assembly is a rate-limiting step in the elongation of WT *A. thaliana* pollen tubes.

RIC3 regulates calcium signaling

In contrast to *RIC4* (Fig. 2 A), *RIC3* OX did not convert the dynamic tip F-actin into a dense network in tobacco pollen tubes (Fig. 4 A). Instead, *RIC3* OX caused loss of tip F-actin and protrusion of the axial actin cables toward the extreme apex of the tobacco pollen tube (Fig. 4 A; 85% tubes, $n = 20$). In WT tubes, the actin cables were absent in the apex (Fu et al., 2001). Furthermore, unlike RIC4 (Fig. 2 A), RIC3-induced tube swelling was not suppressed by either LatB (Fig. 4

A; 88% tubes, $n = 50$) or AtPFN3 (not depicted). Thus, RIC3 has a role distinct from RIC4.

The RIC3-induced actin changes were similar to actin reorganization induced by high $[Ca^{2+}]_{ex}$ in WT pollen tubes (Fig. 4 A). We speculated that RIC3 might regulate Ca^{2+} signals in the tip. Indeed both EGTA (Ca^{2+}-chelating agent) and $LaCl_3$ (which blocks PM-localized inward Ca^{2+} channels) suppressed *RIC3* OX induced growth inhibition and actin reorganization (Fig. 4, A and B; for LaCl3, 82% tubes, $n = 50$; and for EGTA, 86% tubes, $n = 50$, respectively).

To further investigate the connection between RIC3 and Ca^{2+} signaling, we examined Ca^{2+} responses of pollen tubes from *A. thaliana RIC3(RNAi)* and *RIC3* OX lines. We obtained multiple independent homozygous lines having similar phenotypes and altered *RIC3* transcript levels for each of the *RIC3(RNAi)* and *RIC3* OX constructs (Fig. 4 C). WT *A. thaliana* pollen tubes require $[Ca^{2+}]_{ex}$ for growth, likely due to the dependency of tip-focused cytosolic Ca^{2+} ($[Ca^{2+}]_{cyt}$) gradients on an influx of $[Ca^{2+}]_{ex}$ (Obermeyer and Weisenseel, 1991; Pierson et al., 1994). The elongation of WT tubes showed a typical bell shape response to various $[Ca^{2+}]_{ex}$ with 5 mM being optimal (Fig. 4 D). Growth inhibition by high $[Ca^{2+}]_{ex}$ is thought to be due to a negative feedback regulation of Ca^{2+} influxes (Li et al., 1999), but might also involve increased rigidity of apical pectic wall and Ca^{2+}-mediated inhibition of membrane permeability (Robinson, 1977; Holdaway-Clarke et al., 1997). Compared with WT control, *RIC3(RNAi)* inhibited tube growth at lower $[Ca^{2+}]_{ex}$ (0.5 to 5 mM) but promoted growth at high $[Ca^{2+}]_{ex}$ (10 mM), at which *RIC3(RNAi)* tubes elongated to the length of WT tubes grown under the optimal $[Ca^{2+}]_{ex}$ condition (5 mM). *RIC3* OX had a completely opposite effect; it promoted tube elongation at 0.5 mM $[Ca^{2+}]_{ex}$, but inhibited growth at 2 mM or higher $[Ca^{2+}]_{ex}$. These results cannot be explained by any role for RIC3 in mediating cell wall rigidity or general membrane leakiness, but can be satisfactorily explained by its promotion of calcium influxes, which are subject to a negative feedback regulation by high Ca^{2+} levels.

$LaCl_3$ treatments were used to further test RIC3 regulation of $[Ca^{2+}]_{ex}$ influxes. $LaCl_3$ (100 μM) mimicked the effect of *RIC3(RNAi)* on the growth of WT tubes; i.e., optimal growth shifted from 5 to 10 mM of $[Ca^{2+}]_{ex}$ (Fig. 4 E). $LaCl_3$ reversed the effect of *RIC3* OX; i.e., $LaCl_3$-treated *RIC3*-overexpressing tubes mimicked the Ca^{2+} response of WT tubes in the absence of $LaCl_3$ (Fig. 4 E). Furthermore, $LaCl_3$ suppressed the ability of high $[Ca^{2+}]_{ex}$ to rescue pollen tube elongation inhibited by *RIC3(RNAi)* (unpublished data). These results suggest that RIC3 modulates Ca^{2+} signaling by affecting $[Ca^{2+}]_{ex}$ influxes.

RIC3 promotes the accumulation of tip-localized calcium

We next examined whether RIC3 actually influenced the level of cytosolic Ca^{2+} at the tip of the growing pollen tube. We used petunia pollen tubes for Indo-1–based ratio imaging of Ca^{2+} levels, as we have been unsuccessful in pressure microinjecting *A. thaliana* pollen tubes with Ca^{2+} imaging dyes, whereas microinjection of petunia tubes has a high success rate. To confirm that RIC3 likely acts in petunia tubes as predicted from *A. thaliana*, pollen bombarded with *LAT52:RIC3* was cultured at different $[Ca^{2+}]_{ex}$ levels. At 100 μM $[Ca^{2+}]_{ex}$, untransformed pollen did not germinate (0% germination, $n > 200$ grains, three separate experiments), whereas 100% of *LAT52:RIC3* pollen grains germinated ($n = 50$, three separate experiments). At 1 mM $[Ca^{2+}]_{ex}$, 70% of untransformed pollen germinated ($n = 620$), but few *LAT52:RIC3* pollen grains germinated (9%, $n = 45$). These results are consistent with the effect of RIC3 on Ca^{2+}-dependent growth in both tobacco and *A. thaliana* pollen, although the optimal Ca^{2+} level for pollen tube germination and elongation differs among the three species. At 100 μM $[Ca^{2+}]_{ex}$, only *GFP-RIC3*–overexpressing tubes showed a tip-focused Ca^{2+} gradient similar to those of control tubes growing at 1 mM Ca^{2+} (Fig. 4 F). However, *LAT52:RIC3* tubes at 1 mM $[Ca^{2+}]_{ex}$ not only displayed the swollen tip phenotype as predicted from the effect on tobacco tubes, but also displayed an altered tip focused Ca^{2+} gradient, which extended throughout the swollen apex of the tube (Fig. 4 F). Thus, under conditions where control pollen tubes exhibited a normal tip-focused Ca^{2+} gradient, *RIC3* OX led to a delocalized Ca^{2+} gradient and disrupted apical growth. Interestingly, the delocalized Ca^{2+} gradients were not observed in *RIC4*-overexpressing petunia pollen tubes, although they are also swollen at the tips like *RIC3*-overexpressing tubes. Instead, *RIC4* OX led to an apparently reduced tip-focused Ca^{2+} gradient.

RIC3 and RIC4 counteract to control actin dynamics and apical growth

The results described above indicate that ROP1 activates two pathways: (1) a RIC4 pathway promoting apical F-actin assembly, and (2) a RIC3 pathway that modulates $[Ca^{2+}]_{ex}$ influxes required to generate tip-focused $[Ca^{2+}]_{cyt}$ gradients. The ROP-dependent tip F-actin and Ca^{2+} gradients oscillate with the same period but in the different phases (Fu et al., 2001), suggesting a possible functional coordination between the RIC3 and RIC4 pathways. To test this possibility, we cooverexpressed *RIC3* and *RIC4* in tobacco pollen tubes. Surprisingly, this resulted in the recovery of tip growth and normal dynamics of tip F-actin (Table I and Fig. 5 A). This antagonistic effect of RIC3 and RIC4 is unlikely to be due to a competition between these two proteins for binding to ROP1 because RIC3 and RIC4 do not show identical subcellular localization (Wu et al., 2001) and because GFP-RIC4 localization to the apical region of the PM was not altered by RIC3 OX and vice versa, whereas other PM-localized RICs (e.g., RIC1) can remove RIC4 from the PM (unpublished data). Importantly, the ability of RIC3 and RIC4 to counteract each other requires their respective downstream targets, Ca^{2+} and actin (see the next three sections).

A balance between RIC3 and RIC4 is critical for efficient tip growth

The counteraction of the RIC3 and RIC4 pathways suggests that a check and balance between them is important for ROP control of tip growth. Therefore, we next determined whether there was an optimal RIC3/RIC4 ratio for the most efficient polar growth. Varied amounts of *LAT52:RIC3* and *LAT52:RIC4*

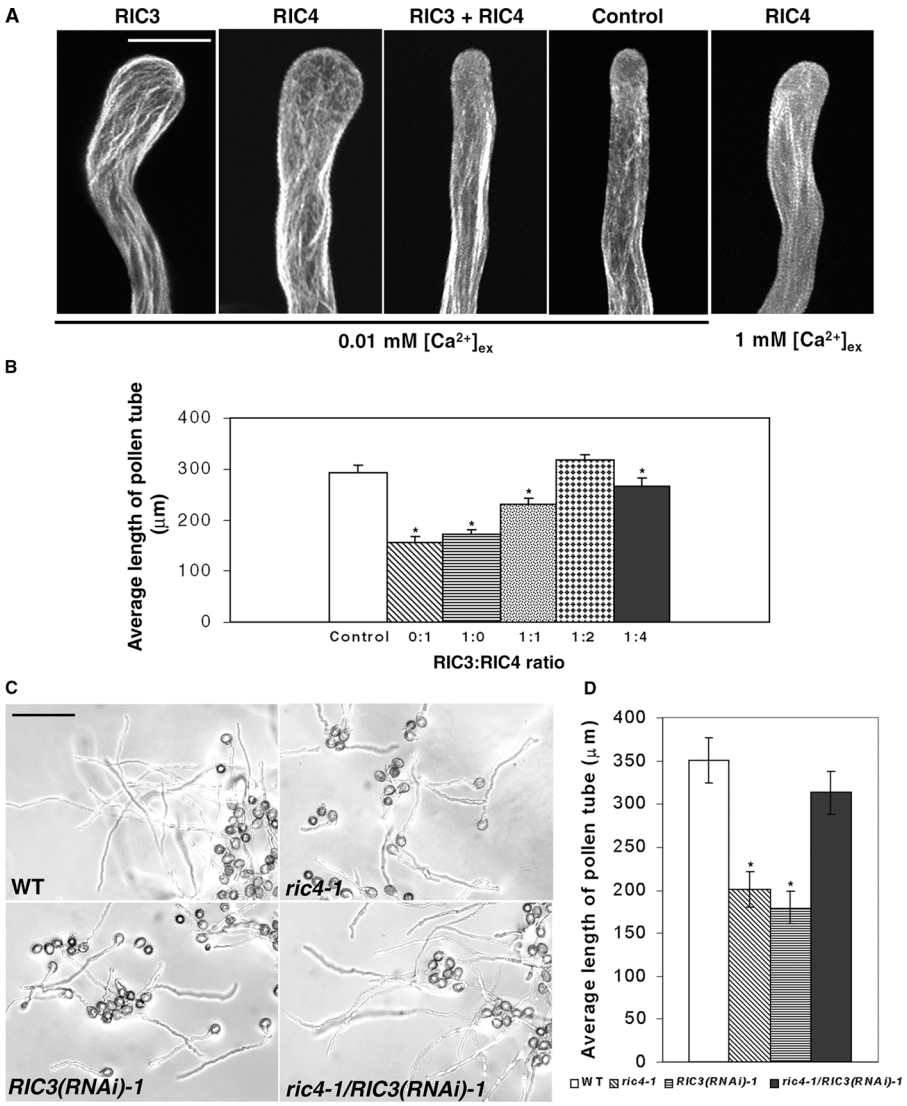

Figure 5. **RIC3 and RIC4 coordinately counteract to control tip growth.** (A) Cooverexpression of RIC3 and RIC4 restored normal tip growth and actin dynamics, similar to high $[Ca^{2+}]_{ex}$ restoration of tip growth in RIC4-overexpressing tubes. *LAT52:GFP-mTalin* was expressed alone (control) or coexpressed with indicated RICs in tobacco pollen tubes cultured in medium containing the indicated $[Ca^{2+}]_{ex}$. All images were projections of 1-μm confocal optical sections. Bar, 20 μm. A video (Video 3) showing the dynamics of tip-localized GFP-mTalin is presented in the online supplemental material. (B) Normal tip growth requires a balance between RIC3 and RIC4. Varied amounts of *LAT52:RIC3* and *LAT52:RIC4* were coexpressed in tobacco pollen tubes. The number in the x axis indicates micrograms of *LAT52:RIC3* or *LAT52:RIC4* plasmid DNA used for bombardment. Data were collected from three individual experiments (~50 tubes per experiment). Asterisk indicates a significant difference from WT at the same data point ($P < 0.01$; *t* test). (C) The RIC3 and RIC4 double knockdown mutant suppressed the pollen tube growth defect in single mutants. *A. thaliana* pollen grains of wild type (Wassilewskija WT), *ric4-1*, *RIC3(RNAi)-1*, and *ric4-1/RIC3(RNAi)-1* were germinated on a growth medium (5 mM Ca^{2+}) and photographed ~6 h after germination. Bar, 120 μm. (D) Quantitative analysis of pollen tube elongation in different *A. thaliana* mutants. The length of pollen tubes as described in C was measured and data were collected from three individual experiments (~100 tubes per experiment). Asterisk indicates a significant difference from WT at the same data point ($P < 0.01$; *t* test).

were coexpressed in tobacco pollen tubes. When either *RIC3* or *RIC4* was overexpressed alone, the tube length was only half that of WT (Fig. 5 B). With fixed *RIC4* DNA amount and *RIC3* DNA amount increasing, the tube length increased. With *RIC3*/*RIC4* = 1:2, optimal tip growth occurred.

Table I. ***RIC3* OX antagonized *RIC4* OX–induced depolarized growth**

	Length[a]	Width[a]	Width/Length
	μm	μm	
GFP	285 ± 13.2	8.8 ± 0.6	0.03
GFP + RIC3	102 ± 8.4	13.6 ± 0.8	0.13
GFP + RIC4	114 ± 10.7	14.2 ± 1.2	0.12
GFP + RIC3 + RIC4	184 ± 12	10.5 ± 2.3	0.06
GFP + RIC4 (1 mM Ca^{2+})	189 ± 6.7	10.9 ± 0.4	0.06

The length and the maximum tip width of tobacco pollen tubes were measured 5–6 h after bombardment. Unless otherwise indicated, all pollen tubes were grown in the presence of 0.01 mM Ca^{2+}. Data were collected from three individual experiments (~50 tubes per experiment), and *t* tests show significant difference between GFP + RIC4 (1 mM Ca^{2+}) and GFP + RIC4 or GFP + RIC3 and RIC4 ($P < 0.05$).
[a]Data are the mean ± SD.

To test whether or not optimal tip growth requires a proper balance of endogenous RIC3 and RIC4, we took advantages of *A. thaliana* LOF *ric3* and *ric4* lines with reduced endogenous expression of respective *RIC3* and *RIC4* genes. Pollen tubes from each of these individual mutants were much shorter than WT tubes at 5 mM optimal $[Ca^{2+}]_{ex}$ (Fig. 5, C and D). However, pollen tubes from the *ric4-1/RIC3(RNAi)-1* double mutant grew almost as long as did WT tubes (Fig. 5, C and D). Furthermore, the elongation of *ric4-1/RIC3(RNAi)-1* tubes showed similar responses to $[Ca^{2+}]_{ex}$ levels as that of WT tubes (Fig. S4, available at http://www.jcb.org/cgi/content/full/jcb.200409140/DC1). Apical F-actin in *ric4-1/RIC3(RNAi)-1* tubes was also normal (Fig. S3). These results clearly demonstrate that it is the balance of counteracting RIC3 and RIC4 that is critical for actin dynamics and tip growth in pollen tubes.

RIC3 acts through Ca^{2+} to promote the disassembly of RIC4-dependent F-actin

Next, we investigated the mechanisms by which the RIC3 and RIC4 pathways counteract and coordinate with each other. We suspected that RIC3-mediated Ca^{2+} signaling might be critical

Table II. **The effect of $LaCl_3$ on the phenotypes of tubes cooverexpressing *RIC3* and *RIC4***

	Length[a]	Width[a]	Width/Length
	μm	μm	
GFP	298 ± 10.6	8.9 ± 0.7	0.03
GFP-RIC4	108 ± 10.4	22.1 ± 0.6	0.20
GFP-RIC4 + $LaCl_3$	112 ± 8.4	20.6 ± 0.8	0.19
GFP-RIC4 + RIC3	160 ± 10.7	16.4 ± 0.5	0.10
GFP-RIC4 + RIC3 + $LaCl_3$	118 ± 12	21.5 ± 2.3	0.18

The length and the maximum tip width of tobacco pollen tube were measured 5–6 h after bombardment. Data were collected from three individual experiments (~50 tubes per experiment) and *t* tests show significant difference between GFP-RIC4 + RIC3 tubes and those treated with $LaCl_3$ ($P < 0.05$).
[a]Data are the mean ± SD.

Table III. **RIC3 and profilin acted additively to suppress *RIC4* OX–induced depolarized growth**

	Length[a]	Width[a]	Width/Length
	μm	μm	
GFP	285 ± 15.3	9.0 ± 0.4	0.03
GFP-RIC4	109 ± 10.4	21.4 ± 0.8	0.20
GFP-RIC4 + AtPFN3	166 ± 5.2	16.9 ± 0.8	0.10
GFP-RIC4 + RIC3	155 ± 5.9	17.7 ± 0.7	0.11
GFP-RIC4 + RIC3 + AtPFN3	278 ± 10.1	14.1 ± 0.3	0.05

The length and the maximum tip width of tobacco pollen tube were measured 5–6 h after bombardment. Data were collected from three individual experiments (~50 tubes per experiment), and *t* tests show that GFP-RIC4 tubes were significantly different from those coexpressing GFP-RIC4 and AtPFN3 ($P < 0.05$) as well as those coexpressing GFP-RIC4 and RIC3 ($P < 0.05$).
[a]Data are the mean ± SD.

for the dynamics of tip F-actin. Ca^{2+} activates several actin disassembly factors, e.g., profilin and gelsolin-like proteins (Kovar et al., 2000; Huang et al., 2004), and elevation of intracellular Ca^{2+} levels causes dramatic actin disassembly in poppy pollen tubes (Geitmann et al., 2000). Interestingly, raising $[Ca^{2+}]_{ex}$ from 0.01 to 1 mM effectively recovered normal tip growth (Table I) and the dynamics of apical F-actin (Fig. 5 A) in *RIC4*-overexpressing tobacco pollen tubes, demonstrating that Ca^{2+} antagonizes RIC4 action. To test if *RIC3*-induced Ca^{2+} elevation in the tip of pollen tubes caused the RIC4-induced disassembly of tip F-actin, we examined the effect of $LaCl_3$ on the counteraction of RIC3 on RIC4. Indeed, $LaCl_3$ treatments of tubes cooverexpressing *RIC3* and *RIC4* induced growth depolarization (Table II) and the formation of a stable apical F-actin network (not depicted) as found in untreated tubes overexpressing *RIC4* alone. These results indicate that RIC3 acts through Ca^{2+} to promote actin dynamics and to antagonize RIC4.

Profilin may be one of the Ca^{2+}-dependent actin disassembling factors linking RIC3-induced Ca^{2+} signals to the dynamics of RIC4-activated F-actin because it partially suppressed *RIC4* OX phenotypes (Table III). Increasing the amount of *PFN3* did not improve its ability to suppress the *RIC4* OX phenotype, suggesting a potential rate-limiting factor required for the function of PFN3 (unpublished data). When *RIC4* was coexpressed with both *PFN3* and *RIC3*, normal pollen tube growth was completely recovered, although the same amount of *RIC3* or *PFN3* alone only partially suppressed the *RIC4* OX phenotype (Fig. 2 and Table III). However, *PFN3* OX did not enhance *RIC3* OX phenotype, suggesting that RIC3-dependent Ca^{2+} may have additional cellular targets such as vesicle fusion. Together, our results indicate that RIC3-mediated $[Ca^{2+}]_{cyt}$, probably acting through profilin and possibly other Ca^{2+}-mediated actin-binding proteins such as gelsolins (Huang et al., 2004), promotes the disassembly of RIC4-dependent apical F-actin, leading to its dynamics during tip growth.

RIC4 acts through F-actin to counteract the RIC3 pathway

RIC4 suppression of tip-localized Ca^{2+} accumulation (Fig. 4 F) suggests that RIC4 may counteract the RIC3-dependent pathway. To test whether or not the RIC4 counteraction of RIC3 is dependent on F-actin, we treated *GFP-RIC3* and *RIC4* cooverexpressing tubes with 5 nM LatB, a concentration that efficiently suppressed *RIC4* OX–induced tube swelling (Fig. 2). *GFP-RIC3* and *RIC4* cooverexpressing tubes showed polarized growth, but LatB-treated tubes cooverexpressing *GFP-RIC3* and *RIC4* exhibited growth depolarization identical to that of *GFP-RIC3*–overexpressing tubes (Table IV). WT tubes treated with 5 nM LatB showed a significant reduction in tube elongation but only a slight growth depolarization (Fig. 2). Therefore, these results suggest that RIC4-mediated F-actin accumulation is required to counteract the RIC3 pathway.

Discussion

In this paper, we have established a novel mechanism for Rho GTPase regulation of actin dynamics and polarized cell growth. ROP1 activates two counteracting pathways that regulate actin assembly and disassembly, respectively. The RIC4 pathway leads to the assembly of apical F-actin, whereas the RIC3-mediated Ca^{2+} signaling is required for the disassembly of this F-actin. A check and balance of these two downstream pathways is critical for efficient polarized growth of pollen tubes, not only because both pathways are required for correct control of actin dynamics but also because they coordinately regulate each other. This paper is also the first to demonstrate an interplay between a Rho GTPase and Ca^{2+} in the control of actin dynamics and to establish a molecular circuitry controlling tip growth in higher eukaryotic cells (Fig. 6).

Table IV. **The effect of LatB on the phenotypes of tubes cooverexpressing *RIC3* and *RIC4***

	Length[a]	Width[a]	Width/Length
	μm	μm	
GFP	302 ± 11.3	9.1 ± 0.3	0.03
GFP-RIC3	110 ± 6.7	18.1 ± 0.6	0.16
GFP-RIC3 + RIC4	164 ± 9.3	14.0 ± 0.5	0.09
GFP-RIC3 + RIC4 + LatB	113 ± 12.7	19.9 ± 0.9	0.18

Pollen tube length and the maximum width of tobacco pollen tube tips were measured 5–6 h after bombardment. Data were collected from three individual experiments (~50 tubes per experiment), and tubes expressing GFP-RIC3 + RIC4 were significantly different from those tubes treated with LatB ($P < 0.05$).
[a]Data are the mean ± SD.

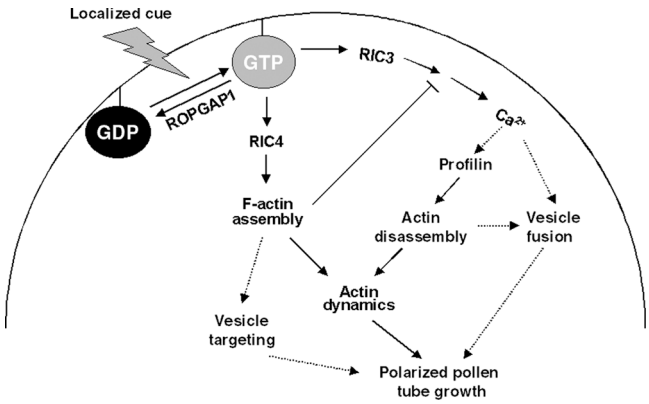

Figure 6. **A model for the ROP GTPase control of actin dynamics and tip growth.** The model predicts that ROP1 is activated at the tip and activates RIC4 and RIC3, which promote the assembly of tip F-actin and lead to the formation of tip-focused $[Ca^{2+}]_{cyt}$ gradients, respectively. The two pathways check and balance to control actin dynamics and tip growth. The RIC4-dependent tip F-actin may target vesicles to the site of exocytosis as well as is required for the proper regulation of the RIC3 pathway. The RIC3-mediated Ca^{2+} promotes the disassembly of the tip F-actin, likely releasing F-actin blockage of vesicle fusion, and may also directly activate vesicle fusion. The dual and antagonistic roles of Rho signaling explain a dilemma for the regulation of exocytosis by Rho GTPase–dependent cortical F-actin; i.e., cortical F-actin is both required for and inhibits exocytosis. The check and balance of the two ROP1 downstream pathways also explain how the extremely polarized growth is coupled with growth oscillation in pollen tubes. Solid arrows indicate steps supported by experimental data described in this paper or elsewhere (Fu et al., 2001), whereas dotted arrows indicate more speculative steps. In addition to profilin, other potential Ca^{2+} sensors such as gelsolin, which might also be involved in RIC3-mediated actin disassembly, are not indicated in the model.

ROP GTPase controls two pathways crucial for tip growth

Our earlier studies have implicated tip-localized ROP GTPases in the regulation of both the generation of tip-focused Ca^{2+} gradients and the assembly of dynamic tip F-actin (Li et al., 1999; Fu et al., 2001). In this paper, we provide evidence that ROPs may coordinate these two cellular events through the activation of the RIC3 and RIC4 pathways, respectively. The LOF mutants for either RIC3 or RIC4 exhibit impaired pollen tube elongation, suggesting that both pathways are required for pollen tube growth. This finding is consistent with the observation that ROP-dependent apical F-actin and tip-focused Ca^{2+} gradients are essential for pollen tube growth (Li et al., 1999; Fu et al., 2001; Hepler et al., 2001; Vidali et al., 2001).

Rho GTPases modulate actin assembly in all eukaryotic organisms, and many Rho effectors controlling this process are conserved in animals and yeast. However, RIC4 does not share sequence similarity to any known Rho GTPase effectors or any other conserved proteins that control actin assembly (e.g., WASP and SCA/WAVE). RIC4 also promotes fine cortical F-actin in *A. thaliana* leaf pavement cells (Fu et al., 2005). The mechanism by which RIC4 promotes actin assembly and the structural nature of RIC4-mediated F-actin remain to be investigated.

Based on the ability of the PM Ca^{2+} channel blocker ($LaCl_3$) to block the effect of RIC3, we favor the hypothesis that RIC3 regulates the tip-localized influx of extracellular Ca^{2+}, which subsequently modulates for the formation of the tip-focused Ca^{2+} gradient. Consistent with this hypothesis are recent studies of ROP2 signaling in the control of root hair tip growth (Molendijk et al., 2001; Jones et al., 2002). ROP2 may act upstream of RHD2, which encodes an NADPH oxidase implicated in the regulation of Ca^{2+} influxes in the control of root hair tip growth (Foreman et al., 2003). RIC3 might regulate NADPH oxidase-mediated Ca^{2+} influxes.

Checks and balances between the RIC3 and RIC4 pathways are critical for spatiotemporal control of tip growth

Our LOF and gain-of-function studies of *RIC4* and *RIC3* have demonstrated a critical role for a check and balance between their actions in the control of apical growth in pollen tubes (Fig. 5). The check and balance is necessary for the dynamics of apical F-actin, which is required for the spatial control of polarized growth in pollen tubes (Fu et al., 2001). Actin dynamics depends on both the assembly and the disassembly of an actin filament. Interestingly, the two ROP downstream pathways (RIC4 and RIC3) promote the assembly and the disassembly of apical F-actin, respectively (Fig. 6). RIC3 promotes the disassembly of F-actin through Ca^{2+}, which may activate profilin and possibly gelsolins. Thus our results demonstrate for the first time that a Rho GTPase controls actin dynamics through two downstream pathways respectively activating actin assembly and disassembly.

The check and balance action of RIC3 and RIC4 may also involve a temporal coordination and regulation of their respective targets, tip Ca^{2+} and F-actin. These two ROP signaling targets coordinately oscillate with the same period but in the different phases during the growth of pollen tubes (Holdaway-Clarke et al., 1997; Messerli et al., 2000; Fu et al., 2001). Thus, the ROP GTPase-orchestrated check and balance between the RIC3 and RIC4 pathways seems to underscore the spatiotemporal control of rapid (up to 1 cm/h) and oscillatory polarized growth in pollen tubes. The check and balance between the RIC3 and RIC4 pathways also entails the antagonistic effect of the RIC4 pathway on the RIC3 pathway. In tobacco and petunia pollen tubes, *RIC3* OX causes depolarized growth due to excess Ca^{2+} accumulation at the tip (Fig. 4 F). The suppression of the *RIC3* OX phenotype by RIC4 is actin dependent, as LatB abolishes this suppression (i.e., *RIC3*- and *RIC4*-coexpressing pollen tubes treated with LatB show the *RIC3* OX phenotype; Table IV). Similarly, WT pollen tubes and root hairs treated with either LatB or cytochalasin D also show tip swelling (Gibbon et al., 1999; Ketelaar et al., 2003). How does the RIC4–actin pathway counteract the RIC3–Ca^{2+} pathway? RIC4-mediated actin assembly appears to inhibit the accumulation of Ca^{2+} at the tip, as suggested by lower $[Ca^{2+}]_{cyt}$ in the tip of *RIC4*-overexpressing tubes (Fig. 4 F). This observation is further supported by the observation that F-actin inhibits a Ca^{2+}-permeable PM channel in *A. thaliana* pollen (Wang et al., 2004). Consequently, RIC4-mediated tip F-actin suppresses *RIC3* OX–induced Ca^{2+} overload in the tip.

Rho GTPase activation of two counteracting pathways: a paradigm for the regulation of actin dynamics, polar cell growth, and cell migration?

It is known that Rho GTPases regulate actin dynamics mainly through the inactivation of actin disassembly and/or promotion of actin assembly in various systems (Ridley, 2001; Etienne-Manneville and Hall, 2002; Pollard and Borisy, 2003). Our observation that ROP GTPase controls actin dynamics by activating both actin assembly and Ca^{2+}-mediated actin disassembly raises an important question: do these dual and antagonistic roles of a Rho GTPase provide a general mechanism for its control of actin dynamics and other cellular processes in various eukaryotic cells? Many observations are consistent with this notion. ROP regulation of root hair tip growth also involves both tip-focused Ca^{2+} gradients and tip-localized dynamic F-actin (Molendijk et al., 2001; Jones et al., 2002). Similarly, fungal hyphal growth is also mediated by Rho GTPases as well as tip-focused Ca^{2+} gradients and F-actin (Heath, 2001).

Rho GTPase modulates neuritogenesis, neurite outgrowth and axon guidance at least partly through the regulation of actin dynamics at the leading edge (Dickson, 2001; Luo, 2002). These processes require cell migration but are also dependent on tip growth as in pollen tubes (Pfenninger et al., 2003). Both of these cellular processes involve Cdc42/Rac promotion of actin assembly through the activation of the Arp2/3 complex and Ca^{2+} transients at the leading edge. Ca^{2+} has been shown to promote actin depolymerization by regulating α-actinin in neuroblast cells (Fukushima et al., 2002). Other actin-binding proteins such as profilin and gelsolin could also be potential targets of Ca^{2+} signals. Importantly, Rho family GTPases promote both entry of extracellular Ca^{2+} and release of intracellular Ca^{2+} stores in several animal cells (Hong-Geller and Cerione, 2000; Mehta et al., 2003). Thus, Cdc42/Rac likely regulates actin dynamics through Ca^{2+}-mediated actin disassembly in neurons and other animal cells in addition to their activation of actin assembly.

Cortical F-actin has a dual and antagonistic role in exocytosis in mammalian cells (i.e., cortical actin targets vesicle but also acts as a barrier to vesicle fusion; Gasman et al., 2004). Cdc42/Rac stimulates exocytosis by activating actin assembly (Gasman et al., 2004) and the IP_3–Ca^{2+} pathway in animal cells (Hong-Geller and Cerione, 2000). In addition to stimulation of vesicle fusion, Cdc42/Rac-mediated Ca^{2+} signals may also promote actin dynamics through their role in actin disassembly. Therefore, Cdc42/Rac stimulation of exocytosis seems to be analogous to ROP GTPase activation of tip growth in pollen tubes in that Rho GTPase signaling coordinately controls two antagonistic downstream pathways: (1) the assembly of cortical F-actin that is necessary for vesicle targeting but blocks vesicle fusion, and (2) Ca^{2+} signaling that may promote both actin disassembly and vesicle fusion.

In conclusion, we have shown that ROP GTPase modulates apical growth and actin dynamics in pollen tubes through two downstream counteracting pathways. This dual and antagonistic role of Rho GTPases may provide a unifying mechanism for their control of various actin dynamic–dependent processes in various eukaryotic systems (e.g., cell migration, neuritogenesis, neuron growth and guidance, and exocytosis).

Materials and methods

Plant materials and growth conditions

A. thaliana ecotypes Columbia and Wassilewskija WT were grown at 22°C in growth rooms with a light regime of 16 h of light and 8 h of dark. *Nicotiana tabacum* plants were grown in growth chambers at 22°C under a light regime of 12 h of darkness and 12 h of light. *Petunia inflata* plants were grown under greenhouse conditions.

DNA manipulation and plasmid construction

For DNA manipulation and plasmid construction, see online supplemental material.

Particle bombardment-mediated transient expression in tobacco and petunia pollen

Mature pollen grains collected from tobacco plants were used for transient expression using a particle bombardment procedure as described previously (Fu et al., 2001). For tobacco, routinely 0.5 mg of gold particles were coated with 0.5 μg (2 μg for petunia) of *LAT52:GFP-RIC* DNA or a mixture of 0.5 μg (2 μg for petunia) of *LAT52:GFP-RICs* DNA with 0.5 μg of other fusion constructs. The pollen grains were incubated for 5 h before observation under an inverted microscope (model TE300; Nikon) as described previously (Fu et al., 2001) or confocal microscope as described in the section Analyses of RIC localization and OX phenotype and F-actin visualization in tobacco pollen tubes.

Drug treatments

For LatB treatments, various concentrations of LatB were included in germination medium using a 5-mM stock solution in DMSO. For $LaCl_3$ and EGTA treatments, a stock solution of 100 and 500 mM was added to the germination medium to a final concentration of 100 μM and 1 mM, respectively.

FRET analysis

FRET analysis was performed using a confocal microscope (model TCS SP2; Leica) equipped with He-Cd laser (used for CFP excitation at 442 nm) and Argon laser (which provides excitation at 514 nm for YFP). The spectral photometric detection system of Leica confocal device allows freely adjusting collection bandwidth for emission signal to minimize bleedthrough signals. Settings for these experiments were as follows: (a) CFP-ROP1 or CFP-DN-rop1: excitation 442 nm, emission 450–490 nm; (b) YFP-RIC3 or YFP-RIC4: excitation 514 nm, emission 525–600 nm; and (c) FRET: excitation 442 nm, emission 560–638 nm. CFP and YFP images were acquired simultaneously and FRET images were acquired separately at the same plane. For photobleaching experiment, a half-dome region at the tip of the pollen tube was selected for scans using the 442-nm laser line. YFP images before and after scans were collected. The ratio of average intensity was calculated. Only cells expressing moderate levels of CFP-ROP and YFP-RIC were studied; high- and low-expressing cells were avoided.

Analyses of RIC localization and OX phenotype and F-actin visualization in tobacco pollen tubes

Approximately 5 h after bombardment, tubes expressing *LAT52:GFP-RIC* were identified using epifluorescence microscopy, imaged, and analyzed as described previously (Fu et al., 2001). The degree of depolarized growth was determined by measuring the diameter of the widest region of the tube and the degree of polar growth was determined by measuring the length of pollen tubes. The subcellular localization of GFP-tagged RIC3 and RIC4 in tobacco pollen tubes was analyzed as described previously (Wu et al., 2001). Transient expression of GFP-mTalin was used to visualize F-actin in tobacco pollen tubes as described previously (Fu et al., 2001). For time-sequence analyses, mid-plane sections of the tip were scanned every 15 s. All confocal images were analyzed using the Metamorph v4.5 and processed using Adobe Photoshop v5.5.

Generation of *RIC3* and *RIC4* RNAi and OX lines and isolation of T-DNA insertional mutants

To screen for *RIC4* T-DNA knockout line from Wisconsin's BASTA collection (Weigel et al., 2000), the gene-specific primer MQKSF and T-DNA left border primer JL-202 were used. To generate *RIC3* OX and *RIC4* OX

constructs, the full-length *RIC4* or *RIC3* cDNA sequence was cloned into pC1300LAT52 vector derived from pCAMBIA1300 (CAMBIA). To generate the *RIC3* RNAi construct, a 407-bp cDNA fragment was amplified using primer 5dsRIC3 and 3dsRIC3. The PCR fragment was ligated into pFGC5941 (ChromDB) to generate a sense construct pFGC5941RIC3sense. The antisense fragment was introduced into pFGC5941RIC3sense. The CaMV *35S* promoter was replaced with *LAT52* after EcoRI–NcoI. *RIC4* RNAi construct was generated similarly using a 360-bp cDNA fragment amplified using primer 5dsRIC4 and 3dsRIC4. The aforementioned constructs were introduced into *Agrobacterium tumefaciens* GV3101 by electroporation and transformed into *A. thaliana* ecotype Columbia. T2 homozygous plants were selected for analysis.

A. thaliana pollen tube growth measurement

Flowers collected from *A. thaliana* plants 2 wk after bolting were used for the examination of pollen tube phenotypes. Pollen was germinated on standard agar medium containing 5 mM Ca^{2+} (with an equal molar ratio of $CaCl_2$ and $Ca[NO_3]_2$) or various concentrations of Ca^{2+} as described previously (Li et al., 1999). Approximately 9–12 h after germination, images of pollen tubes were recorded through a cooled CCD camera (model C4742-95; Hamamatsu) attached on an Eclipse inverted microscope (model TE300; Nikon). The images were analyzed using the MetaMorph v4.5 measurement function. For each transgenic plant, ~100 pollen tubes were chosen randomly for length measurement.

Cytoplasmic Ca^{2+} concentration measurements

Pollen tubes were microinjected with the fluorescent Ca^{2+} indicating dye Indo-1-dextran, and [Ca^{2+}] was monitored by ratio imaging using a confocal microscope (model LSM 410; Carl Zeiss MicroImaging, Inc.) according to Bibikova et al. (1997).

Online supplemental material

Time-lapse videos supplement Figs. 2 and 4 (Videos 1 and 2) and Fig. 5 (Video 3). Videos play at four frames per second. Table S1 shows quantitative analysis of the phenotype of pollen tubes coexpressing ROP1 with various other ROPs. Table S2 lists all primers used in this work. Fig. S1 shows the effects of various ROPs on the localization pattern of GFP-RIC3 or GFP-RIC4. Fig. S2 shows the quantitative analysis of average apical fluorescence intensity in RIC4 OX tubes. Fig. S3 shows alteration of fine F-actin at the tip of pollen tubes in *A. thaliana RIC4* mutants. Fig. S4 shows that pollen tubes of the *ric4-1/RIC3(RNAi)-1* double mutant have normal calcium responses as WT pollen tubes. Online supplemental material is available at http://www.jcb.org/cgi/content/full/jcb200409140/DC1.

We thank Elizabeth Lord for critical reading of this manuscript, the Salk Institute Genomic Analysis Laboratory for providing the sequence-indexed *A. thaliana* T-DNA insertion mutants, David Carter for assistance on FRET analysis, John Fowler for providing pBS-CFP vector, and Albrecht Arnim for providing *pBS35S:YFP* vector.

This work is supported by National Science Foundation grant MCB0111082 to Z. Yand, a Predoctoral Fellowship for Students with Disabilities from the National Institutes of Health to P.E. Dowd, and grants from the U.S. Department of Agriculture and from The Pennsylvania State University Innovative Biotechnology Program to S. Gilroy.

Submitted: 23 September 2004
Accepted: 25 February 2005

References

Aspenstrom, P. 1999. Effectors of the Rho GTPases. *Curr. Opin. Cell Biol.* 11: 95–102.

Bibikova, T.N., A. Zhigilei, and S. Gilroy. 1997. Root hair growth in *Arabidopsis thaliana* is directed by calcium and an endogenous polarity. *Planta.* 203:495–505.

Burbelo, P.D., D. Drechsel, and A. Hall. 1995. A conserved binding motif defines numerous candidate target proteins for both Cdc42 and Rac GTPases. *J. Biol. Chem.* 270:29071–29074.

Dickson, B.J. 2001. Rho GTPases in growth cone guidance. *Curr. Opin. Neurobiol.* 11:103–110.

Etienne-Manneville, S., and A. Hall. 2002. Rho GTPases in cell biology. *Nature.* 420:629–635.

Eyal, Y., C. Curie, and S. McCormick. 1995. Pollen specificity elements reside in 30 bp of the proximal promoters of two pollen-expressed genes. *Plant Cell.* 7:373–384.

Foreman, J., V. Demidchik, J.H. Bothwell, P. Mylona, H. Miedema, M.A. Torres, P. Linstead, S. Costa, C. Brownlee, J.D. Jones, et al. 2003. Reactive oxygen species produced by NADPH oxidase regulate plant cell growth. *Nature.* 422:442–446.

Franklin-Tong, V.E. 1999. Signaling in pollination. *Curr. Opin. Plant Biol.* 2:490–495.

Fu, Y., G. Wu, and Z. Yang. 2001. Rop GTPase–dependent dynamics of tip-localized F-actin controls tip growth in pollen tubes. *J. Cell Biol.* 152: 1019–1032.

Fu, Y., Y. Gu, Z.-L. Zheng, G. Wasteneys, and Z. Yang. 2005. *Arabidopsis* interdigitating cell growth requires two antagonistic pathways with opposing action on cell morphogenesis. *Cell.* 120:687–700.

Fukushima, N., I. Ishii, Y. Habara, C.B. Allen, and J. Chun. 2002. Dual regulation of actin rearrangement through lysophosphatidic acid receptor in neuroblast cell lines: actin depolymerization by Ca^{2+}-alpha-actinin and polymerization by rho. *Mol. Biol. Cell.* 13:2692–2705.

Gasman, S., S. Chasserot-Golaz, M. Malacombe, M. Way, and M.F. Bader. 2004. Regulated exocytosis in neuroendocrine cells: a role for subplasmalemmal Cdc42/N-WASP-induced actin filaments. *Mol. Biol. Cell.* 15: 520–531.

Geitmann, A., B.N. Snowman, A.M. Emons, and V.E. Franklin-Tong. 2000. Alterations in the actin cytoskeleton of pollen tubes are induced by the self-incompatibility reaction in *Papaver rhoeas*. *Plant Cell.* 12:1239–1251.

Gibbon, B.C., D.R. Kovar, and C.J. Staiger. 1999. Latrunculin B has different effects on pollen germination and tube growth. *Plant Cell.* 11:2349–2363.

Heath, I.B. 2001. Regulation of tip morphogenesis by the cytoskeleton and calcium ions. *In* Cell Biology of Plant and Fungal Tip Growth. A. Geitmann, M. Cresti, and I.B. Heath, editors. IOS press, Amsterdam. 37–53 pp.

Hepler, P.K., L. Vidali, and A.Y. Cheung. 2001. Polarized cell growth in higher plants. *Annu. Rev. Cell Dev. Biol.* 17:159–187.

Holdaway-Clarke, T.L., J.A. Feijo, G.R. Hackett, J.G. Kunkel, and P.K. Hepler. 1997. Pollen tube growth and the intracellular cytosolic calcium gradient oscillate in phase while extracellular calcium influx is delayed. *Plant Cell.* 9:1999–2010.

Hong-Geller, E., and R.A. Cerione. 2000. Cdc42 and Rac stimulate exocytosis of secretory granules by activating the IP_3/calcium pathway in RBL-2H3 mast cells. *J. Cell Biol.* 148:481–494.

Huang, S., L. Blanchoin, F. Chaudhry, V.E. Franklin-Tong, and C.J. Staiger. 2004. A gelsolin-like protein from *Papaver rhoeas* pollen (PrABP80) stimulates calcium-regulated severing and depolymerization of actin filaments. *J. Biol. Chem.* 279:23364–23375.

Johnson, M.A., and D. Preuss. 2002. Plotting a course: multiple signals guide pollen tubes to their targets. *Dev. Cell.* 2:273–281.

Jones, M.A., J.J. Shen, Y. Fu, H. Li, Z. Yang, and C.S. Grierson. 2002. The *Arabidopsis* Rop2 GTPase is a positive regulator of both root hair initiation and tip growth. *Plant Cell.* 14:763–776.

Ketelaar, T., N.C. de Ruijter, and A.M. Emons. 2003. Unstable F-actin specifies the area and microtubule direction of cell expansion in *Arabidopsis* root hairs. *Plant Cell.* 15:285–292.

Kost, B., E. Lemichez, P. Spielhofer, Y. Hong, K. Tolias, C. Carpenter, and N.H. Chua. 1999. Rac homologues and compartmentalized phosphatidylinositol 4, 5-bisphosphate act in a common pathway to regulate polar pollen tube growth. *J. Cell Biol.* 145:317–330.

Kovar, D.R., B.K. Drobak, and C.J. Staiger. 2000. Maize profilin isoforms are functionally distinct. *Plant Cell.* 12:583–598.

Li, H., Y. Lin, R.M. Heath, M.X. Zhu, and Z. Yang. 1999. Control of pollen tube tip growth by a Rop GTPase-dependent pathway that leads to tip-localized calcium influx. *Plant Cell.* 11:1731–1742.

Lin, Y., and Z. Yang. 1997. Inhibition of pollen tube elongation by microinjected anti-Rop1Ps antibodies suggests a crucial role for Rho-type GTPases in the control of tip growth. *Plant Cell.* 9:1647–1659.

Lord, E.M. 2003. Adhesion and guidance in compatible pollination. *J. Exp. Bot.* 54:47–54.

Lord, E.M., and S.D. Russell. 2002. The mechanisms of pollination and fertilization in plants. *Annu. Rev. Cell Dev. Biol.* 18:81–105.

Luo, L. 2002. Actin cytoskeleton regulation in neuronal morphogenesis and structural plasticity. *Annu. Rev. Cell Dev. Biol.* 18:601–635.

Malho, R., and A.J. Trewavas. 1996. Localized apical increases of cytosolic free calcium control pollen tube orientation. *Plant Cell.* 8:1935–1949.

McKenna, S.T., L. Vidali, and P.K. Hepler. 2004. Profilin inhibits pollen tube growth through actin-binding, but not poly-l-proline-binding. *Planta.* 218:906–915.

Mehta, D., G.U. Ahmmed, B.C. Paria, M. Holinstat, T. Voyno-Yasenetskaya, C. Tiruppathi, R.D. Minshall, and A.B. Malik. 2003. RhoA interaction with inositol 1,4,5-trisphosphate receptor and transient receptor potential

channel-1 regulates Ca^{2+} entry. Role in signaling increased endothelial permeability. *J. Biol. Chem.* 278:33492–33500.

Messerli, M.A., R. Creton, L.F. Jaffe, and K.R. Robinson. 2000. Periodic increases in elongation rate precede increases in cytosolic Ca^{2+} during pollen tube growth. *Dev. Biol.* 222:84–98.

Miralles, F., G. Posern, A.I. Zaromytidou, and R. Treisman. 2003. Actin dynamics control SRF activity by regulation of its coactivator MAL. *Cell.* 113: 329–342.

Molendijk, A.J., F. Bischoff, C.S. Rajendrakumar, J. Friml, M. Braun, S. Gilroy, and K. Palme. 2001. *Arabidopsis thaliana* Rop GTPases are localized to tips of root hairs and control polar growth. *EMBO J.* 20:2779–2788.

Obermeyer, G., and M.H. Weisenseel. 1991. Calcium channel blocker and calmodulin antagonists affect the gradient of free calcium ions in lily pollen tubes. *Eur. J. Cell Biol.* 56:319–327.

Palanivelu, R., and D. Preuss. 2000. Pollen tube targeting and axon guidance: parallels in tip growth mechanisms. *Trends Cell Biol.* 10:517–524.

Pfenninger, K.H., L. Laurino, D. Peretti, X. Wang, S. Rosso, G. Morfini, A. Caceres, and S. Quiroga. 2003. Regulation of membrane expansion at the nerve growth cone. *J. Cell Sci.* 116:1209–1217.

Pierson, E.S., D.D. Miller, D.A. Callaham, A.M. Shipley, B.A. Rivers, M. Cresti, and P.K. Hepler. 1994. Pollen tube growth is coupled to the extracellular calcium ion flux and the intracellular calcium gradient: effect of BAPTA-type buffers and hypertonic media. *Plant Cell.* 6:1815–1828.

Pollard, T.D., and G.G. Borisy. 2003. Cellular motility driven by assembly and disassembly of actin filaments. *Cell.* 112:453–465.

Ridley, A.J. 2001. Rho GTPases and cell migration. *J. Cell Sci.* 114:2713–2722.

Robinson, K.R. 1977. Reduced external calcium or sodium stimulates calcium influx in *Pelvetia* eggs. *Planta.* 136:153–158.

Vidali, L., S.T. McKenna, and P.K. Hepler. 2001. Actin polymerization is essential for pollen tube growth. *Mol. Biol. Cell.* 12:2534–2545.

Wang, Y.F., L.M. Fan, W.Z. Zhang, W. Zhang, and W.H. Wu. 2004. Ca^{2+}-permeable channels in the plasma membrane of *Arabidopsis* pollen protoplasts are regulated by actin microfilaments. *Plant Physiol.* 136:3892–3904.

Weigel, D., J.H. Ahn, M.A. Blazquez, J.O. Borevitz, S.K. Christensen, C. Fankhauser, C. Ferrandiz, I. Kardailsky, E.J. Malancharuvil, M.M. Neff, et al. 2000. Activation tagging in *Arabidopsis*. *Plant Physiol.* 122:1003–1013.

Wu, G., H. Li, and Z. Yang. 2000. *Arabidopsis* RopGAPs are a novel family of rho GTPase-activating proteins that require the Cdc42/Rac-interactive binding motif for rop-specific GTPase stimulation. *Plant Physiol.* 124: 1625–1636.

Wu, G., Y. Gu, S. Li, and Z. Yang. 2001. A genome-wide analysis of *Arabidopsis* Rop-interactive CRIB motif-containing proteins that act as Rop GTPase targets. *Plant Cell.* 13:2841–2856.

Yang, Z. 2003. GABA, a new player in the plant mating game. *Dev. Cell.* 5:185–186.

Zheng, Z.L., and Z. Yang. 2000. The Rop GTPase switch turns on polar growth in pollen. *Trends Plant Sci.* 5:298–303.

Gu et al. http://www.jcb.org/cgi/doi/10.1083/jcb.200409140

Supplemental materials and methods

RIC3 and RIC4 are specific targets of ROP1 in their control of pollen tube tip growth

Plants (including lower plants such as moss) possess a single subfamily of Rho GTPases, ROP, which is also named RAC in some literature (Winge et al., 2000; Yang, 2002). The *A. thaliana* genome encodes 11 *ROP* genes, which are divided into four phylogenetic groups (I, *ROP8*; II, *ROP9-11*; III, *ROP7*; IV, *ROP1-6*; Zheng and Yang, 2000). We have shown that seven *ROP* genes (*ROP1*, *3*, *5*, *8*, *9*, *10*, and *11*) are expressed in *A. thaliana* pollen (Li et al., 1998; Gu et al., 2003). Among the three most closely related *ROPs* expressed in pollen (*ROP1*, *ROP3*, and *ROP5*), *ROP1* is expressed specifically in pollen to the highest level and has been shown to have a central role in the control of pollen tube tip growth (Li et al., 1998; Gu et al., 2003). ROP3 and ROP5 have evolved from ROP1 through recent gene duplication, share 95% amino acid identity, and 100% similarity to ROP1, and thus are functionally redundant to ROP1 in the control of pollen tube growth (Li et al., 1998; Kost et al., 1999; Li et al., 1999; Zheng and Yang, 2000; Gu et al., 2003). For example, when overexpressed, ROP3 and ROP5 caused the same phenotype and enhanced RIC3 or RIC4 overexpression (OX), as does ROP1 (Kost et al., 1999; Li et al., 1999; unpublished data). *ROP1* transcript levels in pollen are at least 10-fold higher compared with either *ROP3* or *ROP5* (Li et al., 1998). Therefore, ROP1 may have a predominant role in the control of pollen tube growth, whereas ROP3 and ROP5 have a minor role in this aspect.

In contrast to *ROP1*, *ROP8–11* belong to different phylogenetic groups and did not cause tip swelling like ROP1 when overexpressed in cultured tobacco pollen tubes, suggesting that they are not involved in the control of tip growth in cultured pollen tubes. *ROP1* OX was shown to dramatically enhance GFP-RIC1 localization to the PM, whereas ROP8, ROP9, ROP10, or ROP11 did not significantly enhance this GFP-RIC1 localization to the PM (Wu et al., 2001; Gu et al., 2003). Thus, these ROPs have roles distinct from ROP1 function.

To further assess whether or not RIC3 and RIC4 are the specific targets of ROP1 in its control of pollen tube tip growth, the effect of these ROPs on RIC3 and RIC4 localization was examined. *GFP-RIC3* or *GFP-RIC4* was cooverexpressed with each of the following *ROPs*: *ROP1*, *ROP8*, *ROP9*, *ROP10*, *ROP11*. The localization pattern of GFP-RIC3 or GFP-RIC4 was then examined (Fig. S1). As shown previously, *ROP1* cooverexpression dramatically enhanced the apical PM localization of GFP-RIC4 throughout the pollen tube. However, other ROPs did not alter the localization of GFP-RIC4, except that *ROP10* slightly enhanced PM localization of GFP-RIC4 to the subapical region. As previously shown (Wu et al., 2001), GFP-RIC3 by itself was preferentially localized to the apical region of the cytoplasm. Cooverexpression of *ROP1* induced GFP-RIC3 to partially localize to the apical region of the PM, whereas other ROPs did not significantly change the apical localization pattern of GFP-RIC3 (Fig. S1). The ROP1-induced PM localization of GFP-RIC3 was clearly detected in most tubes when we used a high-resolution confocal microscope (SP2; Leica; Fig. S1), but was not clearly detected when we used a low resolution one (model 510; Bio-Rad Laboratories; Wu et al., 2001).

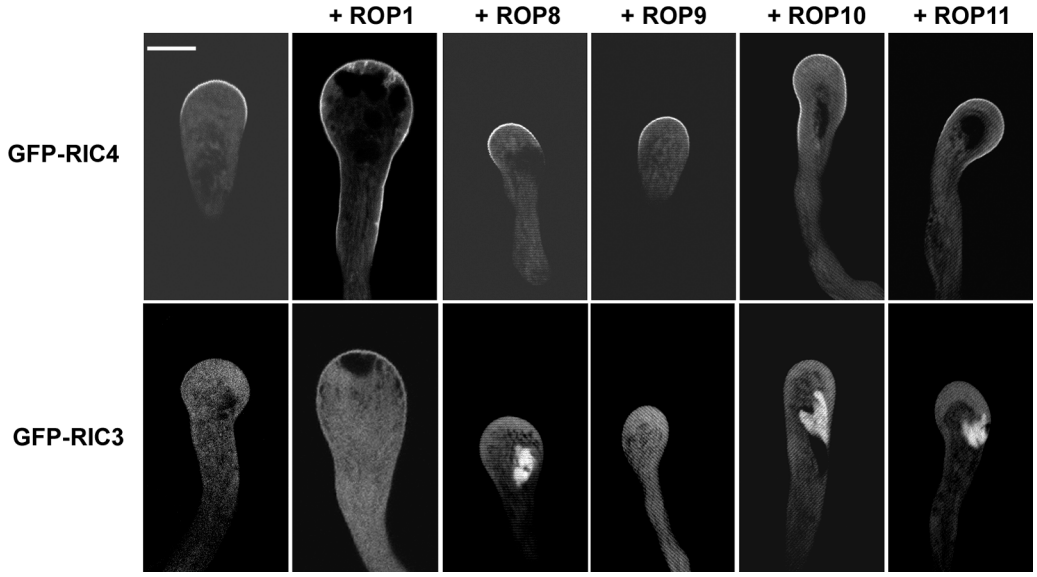

Figure S1. **Effects of various ROPs on the localization pattern of GFP-RIC3 or GFP-RIC4.** *LAT52:GFP-RIC3* or *LAT52:GFP-RIC4* was expressed in tobacco pollen tubes alone or with either *LAT52:ROP1*, *LAT52:ROP8*, *LAT52:ROP9*, *LAT52:ROP10*, or *LAT52:ROP11*, respectively. Tobacco pollen grains were germinated in the medium containing 10 μM Ca^{2+}. 5 h after bombardment, tubes with GFP expression were analyzed by confocal microscopy as described previously (Fu et al., 2001). All images were mid-plane single section of confocal images. Bar = 10 μm.

It was previously shown that *DN-rop1* or *DN-rop5* OX dramatically inhibited pollen tube elongation (Kost et al., 1999; Li et al., 1999). In the full text of this article, we have shown that *DN-rop1* OX eliminated apical localization of GFP-RIC4 and GFP-RIC3 and suppressed *RIC3* and *RIC4* OX phenotypes. However, *DN-rop10* OX did not inhibit pollen tube elongation or change pollen tube morphology; neither did it alter the localization of GFP-RIC3 or GFP-RIC4 or suppress their OX phenotype (unpublished data). Together, these results provide strong evidence that RIC3 and RIC4 are specific ROP1 targets in the control of tip growth but not of other ROPs that are functionally distinct from ROP1.

Table S1. **The phenotype of tubes cooverexpressing *ROP1* and various other *ROPs***

	Length[a]	Width[a]	Width/length
	μm	μm	
GFP-ROP1	313 ± 10.4	17.6 ± 0.9	0.06
GFP-ROP1 + ROP8	259 ± 6.7	22.8 ± 1.5	0.09
GFP-ROP1 + ROP9	239 ± 6.8	24.0 ± 0.6	0.10
GFP-ROP1 + ROP10	251 ± 12.9	25.6 ± 1.2	0.10
GFP-ROP1 + ROP11	218 ± 0.1	20.6 ± 0.1	0.09

Pollen tube length and the maximum width of tobacco pollen tube tips were measured 5–6 h after bombardment.
[a]Data are the mean ± SD.

We next conducted an experiment to further exclude the possibility that counteracting RIC3 and RIC4 pathways are respectively controlled by ROP1 and another ROP functionally distinct from ROP1. As we have shown in the full text of this article, because the RIC3 and RIC4 pathways counteract each other, coexpression of these two RICs resulted in normal pollen tubes. If RIC3 counteracted with RIC4 through two functionally distinct ROPs, ROP1 overexpression phenotype would be suppressed by the other ROP. We cooverexpressed various ROPs with ROP1 using transient expression in tobacco pollen tubes. None of the other functionally distinct ROPs, including ROP8, ROP9, ROP10, and ROP11, suppressed ROP1 OX phenotype (Table S1). Therefore, we conclude that both RIC3 and RIC4 were specifically the functional ROP1 target proteins in the control of pollen tube tip growth.

RIC4-induced quantitative changes in the amount of tip F-actin were reversed by Latrunculin B treatments and RIC3 expression in tobacco pollen tubes

To quantify the effect of RIC4 overexpression on the accumulation of tip F-actin in tobacco pollen tubes, we measured the average intensity of GFP-mTalin fluorescence localized in the extreme 3-μm tip region as previously described (Fu et al., 2001). As shown in Fig. S2, the amount of tip F-actin in RIC4-overexpressing tubes is significantly greater than that in control tubes. Treatments with LatB or coexpression with profilin or RIC3 restored tip F-actin levels to those in the control tubes. Because actin cables protrude to the tip of pollen tubes overexpressing RIC3, the amount of tip F-actin could not be quantified using this approach.

Fine F-actin at the tip of pollen tubes is altered in *A. thaliana ric4* mutants but not in the *ric4-1/RIC3(RNAi)-1* double mutant

To determine the effect of RIC4 OX on the apical F-actin in *A. thaliana* pollen tubes, we first examined the F-actin organization in stably transformed RIC4 OX lines using the traditional actin staining method. The tip F-actin population in the wild-type *A. thaliana* pollen tubes is less abundant compared with that of tobacco pollen tube, which is represented by transient expression of GFP-mTalin. However, RIC4 OX did induce the excessive accumulation of tip F-actin in *A. thaliana* pollen tubes, which is consistent with the results that RIC4 OX lines are less sensitive to the inhibition of pollen tube elongation by LatB than wild type. In contrast, *ric4-1* lines contained much less tip F-actin compare with wild type as we expected (Fig. S3). Interestingly, *ric4-1/RIC3(RNAi)-1* double mutant lines contained a similar amount of tip F-actin as wild type. This data further suggest that the "check and balance" is critical for actin dynamics and tip growth in pollen tubes.

Pollen tubes of the *ric4-1/RIC3(RNAi)-1* double mutant have normal calcium responses compared with wild-type pollen tubes

We further tested if the *ric4-1/RIC3(RNAi)-1* double mutant has any defect in calcium signaling. *A. thaliana* pollen tubes are too small for microinjection to load calcium-sensitive dyes, and thus are not accessible to the measurement of intracellular calcium concentration. Therefore, we examined pollen tube growth responses to different $[Ca^{2+}]_{ex}$ in the above line. When $[Ca^{2+}]_{ex}$ranged from 0.5 to 10 mM, the *ric4-1/RIC3(RNAi)-1* double mutant behaved similarly to wild type (Fig. S4). These results are consistent with the observation that RIC4-dependent actin antagonizes RIC3-mediated calcium signaling and thus further support the check and balance hypothesis.

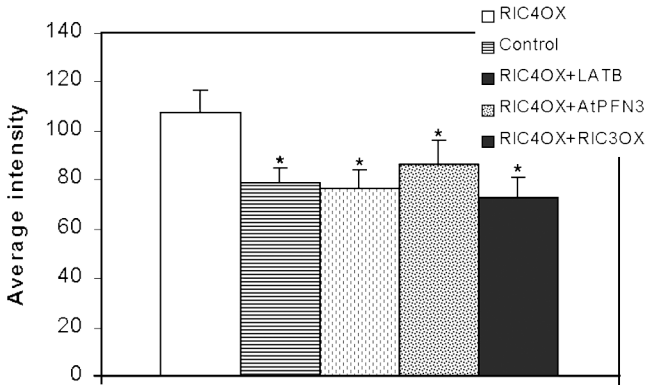

Figure S2. **Quantitative analysis of average apical florescence intensity in RIC4 OX tubes.** The average GFP intensity in a region of the apical dome (~5 μm from the extreme apex) were determined as described previously (Fu et al., 2001). Images were collected from more than 20 tubes for each data point. Asterisk indicates a significant difference from wild type at the same data point ($P < 0.05$; *t* test).

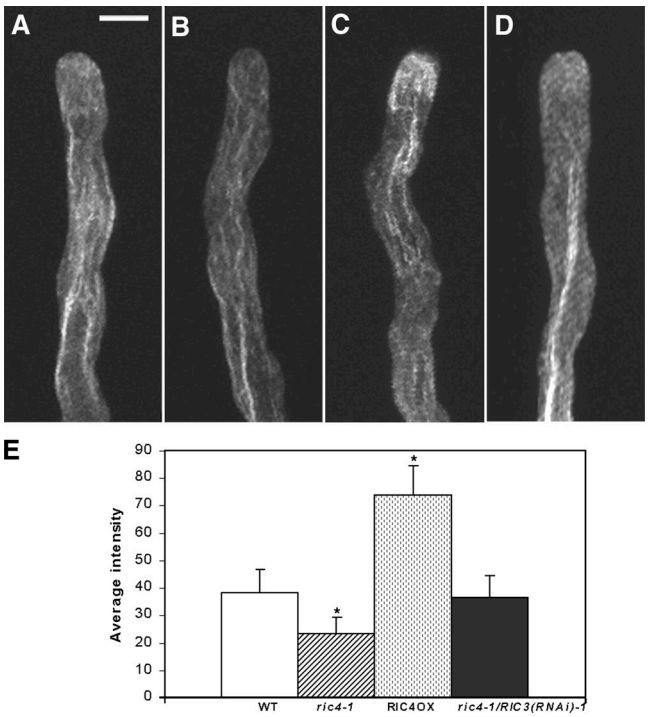

Figure S3. **Fine F-actin at the tip of pollen tubes is altered in *A. thaliana RIC4* mutants.** To determine the effect of RIC4 on the apical F-actin in *A. thaliana* pollen tubes, we stained F-actin in pollen tubes from *ric4-1* mutant and RIC4 OX lines. The actin staining procedure was adopted from Derksen et al. (2002) with some modifications. Pollen grains from different *A. thaliana* lines were collected and germinated on semi-solid medium containing 0.01% H_3BO_3, 1 mM $CaCl_2$, 1 mM $Ca(NO3)_2$, 1 mM $MgSO_4$, 18% sucrose, and 0.5% agar for 10 h. Pollen tubes grown on agar medium were fixed for 4 h in a mixture of 3% freshly made PFA in 18% sucrose, 100 mM potassium phosphate buffer, pH 7.2, and 10 mM EGTA. After fixation, pollen tubes were rinsed three times in 5% DMSO, 16% sucrose, 5 mM EGTA, and 100 mM potassium phosphate buffer, pH 7.2. Actin filaments were labeled with Alexa 488-phalloidin (Molecular Probes) at the final concentration of 10 μM for ~1 h. Actin filaments were visualized using confocal microscope (Bio-Rad Laboratories) as described in Materials and methods except that 0.5-μm optical sections were collected. All images were projections of 1-μm confocal optical sections. Bar = 10 μm. A, wild type; B, *ric4-1*; C, *RIC4* OX; D, *ric4-1/RIC3(RNAi)-1*. As shown in Fig. S3, wild-type *A. thaliana* pollen tubes displayed typical axial F-actin cables ending near the tip where fine F-actin was observed. This fine tip F-actin was dramatically reduced in *ric4-1* tubes but greatly increased in *RIC4* OX tubes. (E) Quantitative analysis of average apical florescence intensity in wild type, *ric4-1*, *RIC4* OX, and *ric4-1/RIC3(RNAi)-1* pollen tubes. Measurement was performed as described in Fig. S2. Asterisk indicates a significant difference from WT at the same data point ($P < 0.05$; *t* test).

Construction of plasmids and summary of primers used

Plasmids used for transient expression in pollen tubes including *LAT52:GFP-RIC3*, *LAT52:GFP-RIC4*, *LAT52:RIC3*, *LAT52:RIC4*, *LAT52:DN-ROP1*, *LAT52:ROPGAP1*, *LAT52:GFP-mTalin*, and *LAT52:AtPFN3* were constructed in *LAT52:GFP* or *LAT52* vector as described previously (Fu et al., 2001; Wu et al., 2001). The *ROP8* or *ROP9* cDNA fragment was subcloned into *LAT52* vector using BamHI–SacI from pGEX-ROP8 and pGEX-ROP9, respectively. *LAT52:ROP10* and *LAT52:ROP11* constructs were generated by PCR amplification using primers as indicated in Table S2 and subcloned into *LAT52* vector. *DNROP10* cDNA fragment was subcloned into LAT52 vector using XbaI–SacI from *pGEM-DNROP10* (Zheng et al., 2002) to generate LAT52:DNROP10. To generate *LAT52:YFP* vectors, the CaMV *35S* promoter was replaced with *LAT52* using XhoI–EcoRI in the pBS35S:YFP (a gift from A. Arnim, University of Tennessee, Knoxville, TN). The *RIC3* cDNA fragment was excised using BglII–SstI from *LAT52:GFP-RIC3* and cloned as a translational fusion to the COOH terminus of YFP in *LAT52:YFP*. *RIC4* cDNA fragment was excised using BamHI–SstI from pBS-RIC4 and cloned as a translational fusion to the COOH terminus of YFP in *LAT52:YFP*. To generate *LAT52:CFP* vectors, *CFP* DNA fragment was excised using NcoI–KpnI from pBS-CFP (a gift from J. Fowler, Oregon State University, Corvallis, OR) and cloned into *LAT52* vector. *ROP1* and *DN-ROP1* DNA fragments were excised using BglII–SstI and KpnI–SstI, respectively, and cloned as a translational fusion to the COOH terminus of CFP in *LAT52:CFP*. AtPFN3 was amplified using AtPFN3F and AtPFN3R and cloned to *LAT52* vector.

Table S2. **Primers used in generating various constructs**

Primer name	Sequence
AtPFN3F	5′-ccatgggatccatgtcgtggcaaacttacgtt-3′
AtPFN3R	5′-gagctcggtaccctagagaccctgttcgagg-3′
RIC4H37D/H40D	5′-cgtccggattcccaaccgatgtccgatacatcttt-3′
RIC3H37D/H40D	5′-cggatccgatgtcggcgacatcctttac-3′
MQKSF	5′-gggatccatgagagatagaatggag-3′
JL202	5′-cattttataataacgctggcggacatctac-3′
5dsRIC3	5′-gtcctagaggcgcgccaacgagaatggtcaagta-3′
3dsRIC3	5′-cgggatccatttaaatgtcttcttcattatagc-3′
5dsRIC4	5′-gctctagaggcgcgcctcaagtgttgctttg-3′
5dsRIC4	5′-cgggatccatttaaatagcagcggctgcaagcaa-3′
ROP10F	5′-gcagatctatggcttcgagtgcttca-3′
ROP10R	5′-tgcgagctctcaattcttcccacacag-3′
ROP11F	5′-cgcgatatcatggcttcaagtgcttca-3′
ROP11R	5′-tgcgagctctcaatgccgagtcactat-3′

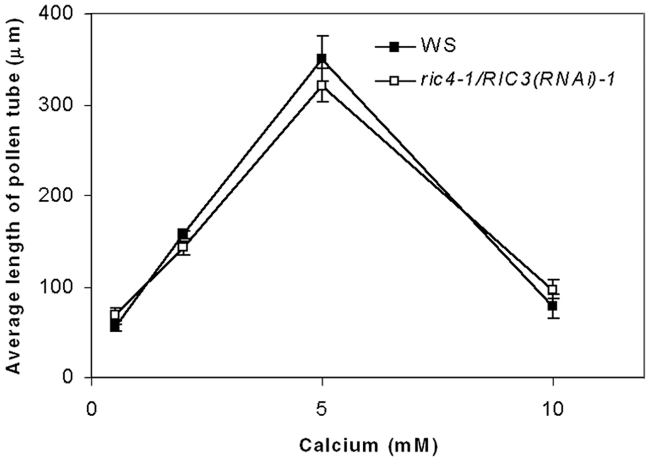

Fig. S4. **Pollen tubes of the *ric4-1/RIC3(RNAi)-1* double mutant have normal calcium responses as WT pollen tubes.** Pollen grains from wild-type plants (WS) and plants homozygous for *ric4-1/RIC3(RNAi)-1* were germinated overnight on a medium containing 0.5, 2, 5, or 10 mM Ca^{2+}. Data were collected from three individual experiments (≥100 tubes per experiment).

PCR-based site-directed mutagenesis was used to create point mutations for RIC3 and RIC4. RIC3 or RIC4 H37D/H40D mutant was generated using primer RIC3H117D/H110D and RIC4H37D/H40D, respectively. Both mutant constructs were then cloned as a translational fusion to the COOH terminus of GFP behind the *LAT52* promoter or directly cloned to *LAT52* vector.

References

Derksen, J., B. Knuiman, K. Hoedemaekers, A. Guyon, S. Bonhomme, and E.S. Pierson. 2002. Growth and cellular organization of *Arabidopsis* pollen tubes in vitro. *Sexual Plant Reproduction.* 15:133–139.

Fu, Y., G. Wu, and Z. Yang. 2001. Rop GTPase-dependent dynamics of tip-localized F-actin controls tip growth in pollen tubes. *J. Cell Biol.* 152:1019–1032.

Gu, Y., V. Vernoud, Y. Fu, and Z. Yang. 2003. ROP GTPase regulation of pollen tube growth through the dynamics of tip-localized F-actin. *J. Exp. Bot.* 54:93–101.

Kost, B., E. Lemichez, P. Spielhofer, Y. Hong, K. Tolias, C. Carpenter, and N.H. Chua. 1999. Rac homologues and compartmentalized phosphatidylinositol 4, 5-bisphosphate act in a common pathway to regulate polar pollen tube growth. *J. Cell Biol.* 145:317–330.

Li, H., Y. Lin, R.M. Heath, M.X. Zhu, and Z. Yang. 1999. Control of pollen tube tip growth by a Rop GTPase-dependent pathway that leads to tip-localized calcium influx. *Plant Cell.* 11:1731–1742.

Li, H., G. Wu, D. Ware, K.R. Davis, and Z. Yang. 1998. Arabidopsis Rho-related GTPases: differential gene expression in pollen and polar localization in fission yeast. *Plant Physiol.* 118:407–417.

Winge, P., T. Brembu, R. Kristensen, and A.M. Bones. 2000. Genetic structure and evolution of RAC-GTPases in *Arabidopsis thaliana*. *Genetics.* 156:1959–1971.

Wu, G., Y. Gu, S. Li, and Z. Yang. 2001. A genome-wide analysis of *Arabidopsis* Rop-interactive CRIB motif-containing proteins that act as Rop GTPase targets. *Plant Cell.* 13:2841–2856.

Yang, Z. 2002. Small GTPases: versatile signaling switches in plants. *Plant Cell.* 14(Suppl):S375–S388.

Zheng, Z.L., and Z. Yang. 2000. The Rop GTPase switch turns on polar growth in pollen. *Trends Plant Sci.* 5:298–303.

Zheng, Z.-L., M. Nafisi, H. Li, A. Tam, D.N. Crowell, S.N. Chary, J. Shen, J. I. Schroeder, and Z. Yang. 2002. Plasma membrane-associated ROP10 small GTPase is a specific negative regulator of abscisic acid responses in *Arabidopsis*. *Plant Cell.* 14: 2787–2797.